Discovery, Synthesis, and Biological Evaluation of Novel SMN Protein Modulators

Jingbo Xiao,[*,†] Juan J. Marugan,[*,†] Wei Zheng,[†] Steve Titus,[†] Noel Southall,[†] Jonathan J. Cherry,[‡,§] Matthew Evans,[‡] Elliot J. Androphy,[‡,§] and Christopher P. Austin[†]

[†]NIH Chemical Genomics Center, National Human Genome Research Institute, National Institutes of Health, 9800 Medical Center Drive, Rockville, Maryland 20850, United States

[‡]Department of Medicine, University of Massachusetts Medical School, 364 Plantation Street, LRB 328, Worcester, Massachusetts 01605, United States

Ⓢ Supporting Information

ABSTRACT: Spinal muscular atrophy (SMA) is an autosomal recessive disorder affecting the expression or function of survival motor neuron protein (SMN) due to the homozygous deletion or rare point mutations in the survival motor neuron gene 1 (SMN1). The human genome includes a second nearly identical gene called SMN2 that is retained in SMA. SMN2 transcripts undergo alternative splicing with reduced levels of SMN. Up-regulation of SMN2 expression, modification of its splicing, or inhibition of proteolysis of the truncated protein derived from SMN2 have been discussed as potential therapeutic strategies for SMA. In this manuscript, we detail the discovery of a series of arylpiperidines as novel modulators of SMN protein. Systematic hit-to-lead efforts significantly improved potency and efficacy of the series in the primary and orthogonal assays. Structure–property relationships including microsomal stability, cell permeability, and in vivo pharmacokinetics (PK) studies were also investigated. We anticipate that a lead candidate chosen from this series may serve as a useful probe for exploring the therapeutic benefits of SMN protein up-regulation in SMA animal models and a starting point for clinical development.

8l AC$_{50}$ = 77 nM (709%)

8m AC$_{50}$ = 31 nM (576%)

9a AC$_{50}$ = 12 nM (325%)
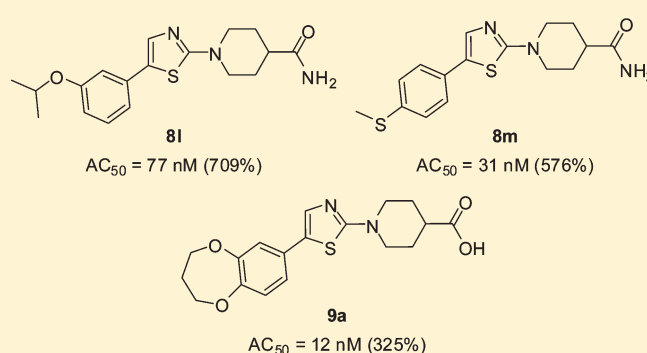
■ INTRODUCTION

Spinal muscular atrophy (SMA), an inherited autosomal neurodegenerative disease, is the leading genetic disorder affecting infant mortality.[1] SMA is a relatively "common" rare disease, affecting approximately 1 in 6000 newborns. Approximately 1 in 40 individuals are genetic carriers.[2] Clinically, there are four types of SMA (types I, II, III, and IV). The determination of the type of SMA is based upon the physical milestones achieved. Usually, children with the most severe form of the disease (type 1; Werdnig–Hoffmann disease) die before the age of two years in the absence of supportive respiratory care.[3] In fact, SMA is the number one genetic cause of death in children under the age of two, and many of those children who make it through infancy are confined to wheelchairs for their entire lives. There is currently no cure or effective therapy for SMA.

SMA is caused by deficiency in survival motor neuron (SMN) protein due to homozygous mutations or deletion of the survival motor neuron 1 telomeric gene (SMN1) that is located on chromosome 5q13.[4] The SMN protein is expressed in all tissues, although there are broad variations regarding levels. Deficiencies in SMN lead to degeneration and dysfunction of alpha motor neurons in the anterior horn of the spinal cord. Studies of the correlation between SMA severity and the amount of SMN protein have shown an inverse relationship.[5] Humans possess an additional paralogous gene, survival motor neuron 2 (SMN2), a centromeric copy gene that differs from the SMN1 gene at a critical nucleotide at position six in exon 7 (C-T).[6] While full length 38 kDa SMN protein can be produced from the transcription of both SMN1 and SMN2 genes, the small variation in the C−T nucleotide has important consequences for alternative splicing of the SMN2 transcript. The pre-mRNA transcripts from SMN1 gene produce full-length mRNA with nine exons encoding full-length of SMN protein, while the C- to T- transition at position six in exon 7 of SMN2 induces mostly alternative pre-mRNA splicing lacking exon 7, which results in the truncated SMN protein (termed as SMNΔ7) as its major product. SMNΔ7 protein has a reduced ability to self-oligomerize, leading to protein instability and rapid degradation.[7] SMN2 has been genetically validated as a target for SMA therapy, and there is a striking correlation between SMA type and SMN2 gene copy numbers.[8] From the functional point of view, SMN associates

with proteins Gemin 2, Gemin 3, and Gemin 4, forming a large complex that plays a role in snRNP assembly, pre-mRNA splicing, and transcription.[9]

There are several SMA therapeutic strategies under investigation, including gene therapy,[10] antisense oligonucleotides (ATO),[11] and stem cells.[12] However, increasing SMN protein levels by altering expression of the SMN2 mRNA by small molecules has been proposed as a promising potential therapeutic strategy for SMA. Over the past several years, several classes of small molecules have been identified that increase SMN transcript and/or protein levels in SMA patient-derived cell lines through a variety of mechanisms.[13] Chang et al. reported that sodium butyrate effectively increased the amount of exon 7-containing SMN protein in SMA lymphoid cell lines by changing the alternative splicing pattern of exon 7 in the SMN2 gene. In vivo, sodium butyrate treatment of SMA-like mice resulted in increased expression of SMN protein in motor neurons of the spinal cord and resulted in significant improvement of SMA clinical symptoms.[14] Sodium 4-phenylbutyrate (PBA), an analogue of sodium butyrate, was also found to increase SMN expression in vitro. PBA has a much longer half-life time (1.5 h) in human serum compared with sodium butyrate (6 min), which suggested that PBA, also due to its favorable pharmacological properties, could be a candidate for the treatment of SMA.[15] The FDA approved antineoplastic drug hydroxyurea was recently reported as a candidate SMA therapeutic due to its strong safety profile, high pediatric bioavailability, and its known gene up-regulation.[16] Other bioactive agents,[17] such as valproic acid,[18] aclarubicin (aclacinomycin A),[19] tobramycin and amikacin,[20] Trichostatin A (TSA),[21] suberoylanilide hydroxamic acid (SAHA),[22] EIPA [5-(N-ethyl-N-isopropyl)-amiloride],[23] LBH589,[24] and (E)-Resveratrol,[25] have been shown to increase levels of exon 7-containing SMN transcript and/or overall SMN protein. All of these repurposed agents have significant liabilities that include gastrointestinal bleeding, short half-life in human serum, high toxicity, and lack of target specificity; additionally, valproic acid, PBA, and hydroxyurea were not therapeutic in human trials. Lunn et al. identified indoprofen as having an effect on full length SMN2 expression in a cell-based reporter assay that up-regulated the SMN protein through a cyclooxygenase-independent mechanism, but it was not potent (AC$_{50}$ >1 μM) and increased protein expression by only 13% (p-value <0.0139).[26] Recently, a tetracycline compound, PTK-SMA1, was found to have the activity to promote SMN2 exon 7 splicing. However, this compound could not penetrate the blood—brain barrier or increase SMN protein concentration in the central nervous system.[27] Another previous high-throughput screen identified two novel chemical series as HDAC inhibitors that can modulate reporter activity in a cell-based SMN2 promoter assay.[28] Another quinazoline series probe, identified as D156844, targets DcpS, which appears to modulate SMN protein levels by stabilizing the SMN2 mRNA transcript.[29] Oral administration of D156844 significantly increased the mean lifespan of SMNΔ7 SMA mice by approximately 21—30% when given prior to motor neuron loss.[30] After removal of the compound's off-target activity, reducing its toxicity and improving its potency and brain permeability, it produced the current clinical candidate, D157495.[31] However, it has not been shown whether this series of molecules acts specifically on SMN2 mRNA transcript stability or what the safety profile of this molecule might be.[32]

We are particularly interested in identifying small molecules that can increase the level of SMN transcript harboring the full length of SMN protein for the therapeutic goal. This may be achieved by modulating splicing, increasing the level of transcript
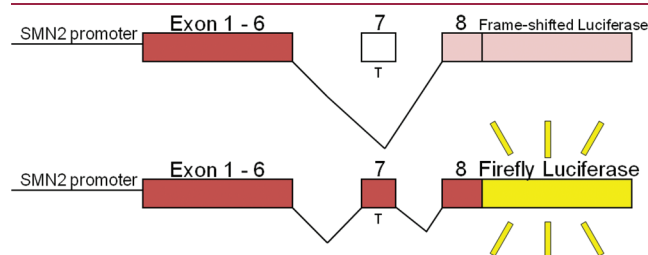

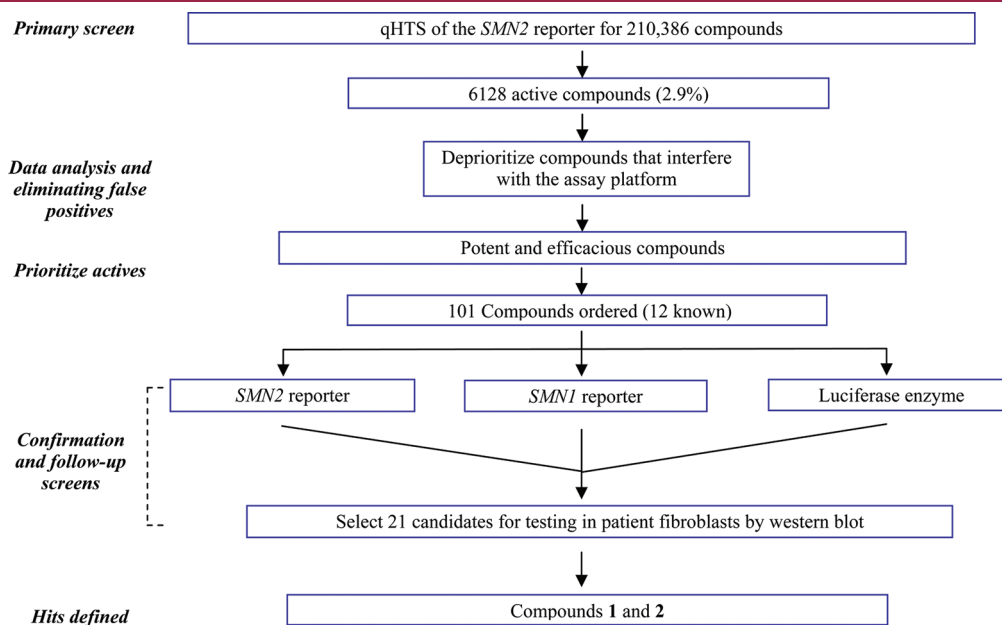**Figure 1.** SMN2-luciferase reporter assay.

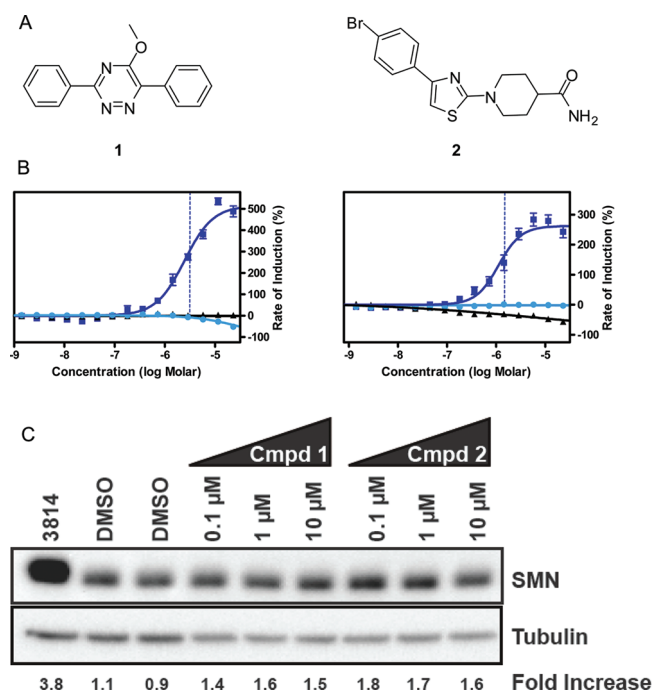**Figure 2.** Overview of screening and hits selection process.

Figure 3. (A) Chemical structures of **1** and **2** from qHTS. (B) Activity of compounds **1** and **2** in *SMN1* (cyan) and *SMN2* (blue) reporter assays, indicating the rate of SMN induction (ROI) at different concentrations, and luciferase inhibition assay (black). (C) Quantification by Western blot of SMN levels after treatment with compounds **1** and **2** at different concentrations, as indicated.

produced, or stabilizing the SMN protein. To achieve this goal of looking for molecules able to elevate SMN levels by any of those mechanisms, we developed a new high-throughput screening methodology that allows us to test a large number of compounds in a quantitative manner. In this manuscript, we present some of the results of our screening and optimization campaign.

■ RESULTS AND DISCUSSION

qHTS Results. Using a luciferase reporter gene assay that combines the promoter and splicing based cassettes in tandem with the major portion of the native *SMN2* cDNA with luciferase, we were able to screen for modulators of all of these mechanisms in a high-throughput manner. Earlier screening assays for SMA only targeted compounds that either stimulate the *SMN2* promoter or decrease exon 7 skipping. In this reporter assay, the *SMN2* promoter drives expression of luciferase reporter that is fused to an SMN splicing reporter (Figure 1). By including our SMN splicing cassette,[33] luciferase is only expressed when exon 7 is included in the mRNA transcript and the full-length SMN protein is generated. This new assay can identify compounds that increase SMN protein levels by three mechanisms: modulating alternative splicing of *SMN2* exon 7, increasing transcription from the *SMN2* promoter or, due to the presence of the native *SMN2* cDNA, and stabilizing the SMN protein. The assay measures the luminescent signal produced by luciferase, and compounds that increase luminescence are flagged as potential actives.

We performed quantitative high-throughput screen (qHTS)[34] using this cell-based *SMN2*-luciferase reporter assay to identify compounds that increase expression of the full-length SMN
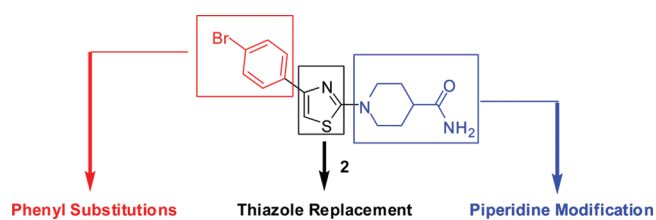

Figure 4. SAR strategy.

protein. The NIH Molecular Libraries Small Molecule Repository (MLSMR),[35] containing 210386 compounds, was screened in the primary assay during the course of this screen campaign (Figure 2). We tested 1229 1536-well plates in the primary screen. The signal to background averaged 9-fold, and the average Z' for the screen was 0.47 ± 0.12, excluding 8 plates which failed visual quality control. 6128 compounds were found to give significant concentration−responses in the primary screen. Compounds were deprioritized for confirmation if they were suspected to interfere with assay readout or cellular viability using internal SAR data from other related assays of the MLPCN using the same chemical library.[36] Recently, it has been brought to our attention that certain classes of luciferase inhibitors can stabilize the luciferase protein and therefore appear as compounds that are able to increase the signal.[37] Compounds that act as luciferase inhibitors could score in the *SMN2* assay as false positives due to this phenomenon. Indeed, more than 98% of hits in the primary screen were identified as luciferase inhibitors, which presumably stabilized the *SMN2*-luciferase fusion protein and prevented cellular degradation, although this has not been explicitly proven. Select samples active in the primary screen were obtained in DMSO stock solutions from the MLSMR and/ or as powders from compound vendors to confirm activity in the original assay. A homologous cell line harboring the *SMN1* gene fused to luciferase was used as a counterscreen. The *SMN1* reporter recapitulates the splicing pattern typically seen with the endogenous *SMN1* gene and predominately includes exon 7. Follow-up compounds that exhibit increased signal in the *SMN1* cell line were flagged as nonspecific activators (i.e., transcription or protein stability). Purified luciferase enzyme was used in another counterscreen of the active compounds to filter out the potential false positives. A complete cheminformatics analysis of the follow-up screening data included chemotype clustering, singleton identification, and structural considerations, including physical properties and optimization potential. In addition, potency range, maximum response, and the curve class[38] were also considered. Ultimately, this analysis led to selection of 21 candidates for further confirmation. The results of this qHTS screening campaign are detailed in Figure 2.

Ideally, compounds modulating SMN protein production in the *SMN2*-luciferase reporter line would also modulate SMN protein production in primary fibroblasts directly derived from SMA individuals. Therefore, 21 compounds representing the diverse set of chemotypes[39] were tested in a SMA-derived patient fibroblast assay for up-regulation of SMN protein production by Western blot in a luciferase-free setting. Ultimately, this campaign led us to focus on two lead series represented by the 5-methoxy-3,6-diphenyl-1,2,4-triazine (**1**) and 1-(4-(4-bromophenyl)thiazol-2-yl)piperidine-4-carboxamide (**2**), which were able to increase the luciferase signal in the *SMN2* reported assay and increase SMN protein production in a dose dependent manner in the

**Scheme 1. Synthesis of the Hit Compound 2 and 4-Arylthiazolyl Piperidine Analogues**[a]
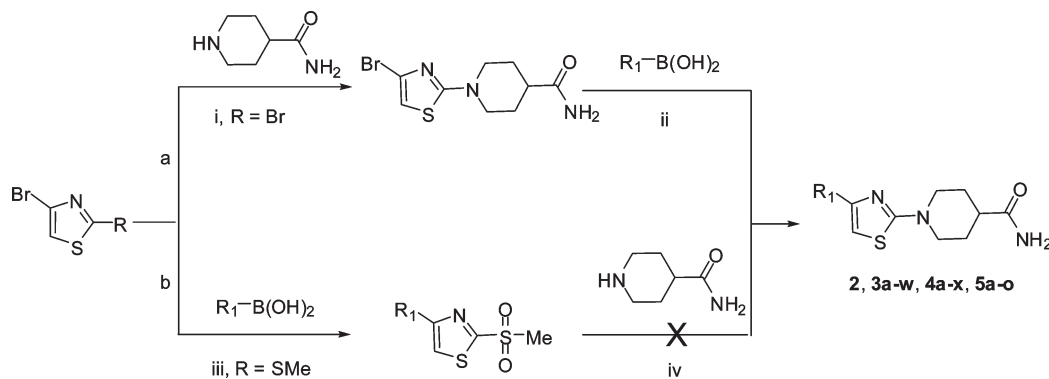
[a] Conditions and reagents: (i) triethylamine, μW, 100 °C; (ii) arylboronic acids or pinacol esters, 2.0 N Na$_2$CO$_3$, 5% Pd(PPh$_3$)$_4$, μW, 100 °C; (iii) (a) 4-bromophenylboronic acid, 2.0 N Na$_2$CO$_3$, 5% Pd(PPh$_3$)$_4$, μW, 100 °C, (b) MCPBA; (iv) triethylamine, μW, 100 °C.

Scheme 2. Modifications at the Thiazole Core Template[a]
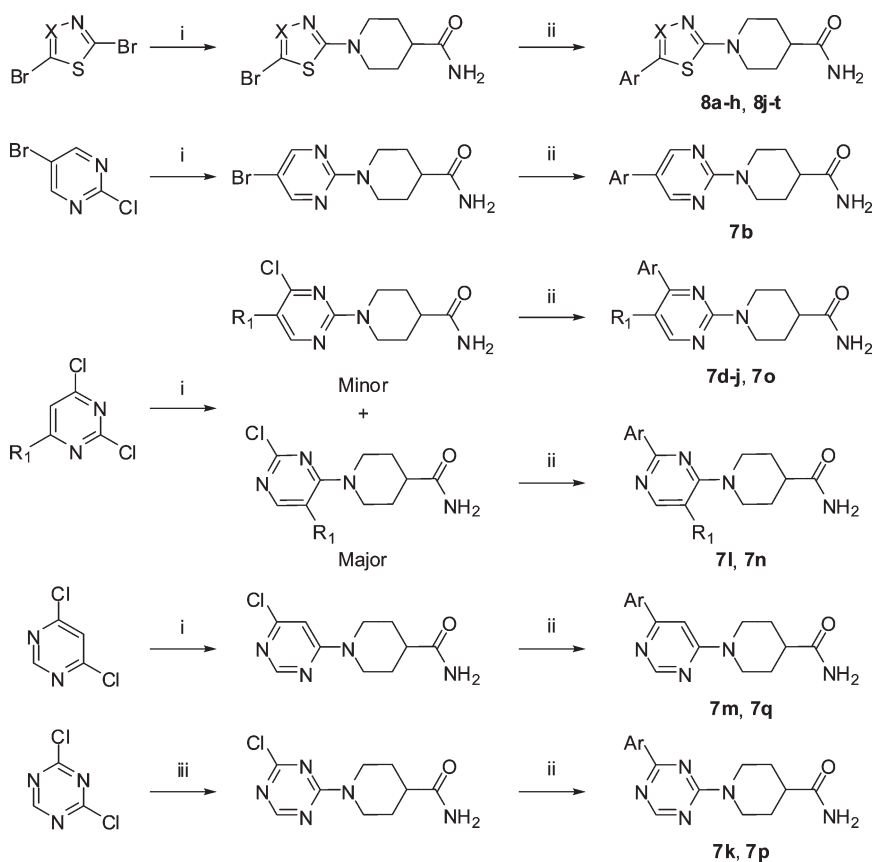
[a] Conditions and reagents: (i) piperidine-4-carboxamide, triethylamine, μW, 100 or 120 °C; (ii) arylboronic acids or pinacol esters, 2.0 N Na$_2$CO$_3$, 5% Pd(PPh$_3$)$_4$, μW, 100 °C; (iii) piperidine-4-carboxamide, N,N-diisopropylethylamine, 0 °C.

Western blot (Figure 3). In addition, although we do not know their specific mechanism of action, we noticed that two active compounds **1** and **2** appear to have distinct mechanisms of action. Compound **1** increased the expression of *SMN2* and did not affect the expression of *SMN1*. On other hand, compound **2** increased the expression of *SMN2* but reduced the expression of *SMN1*. This reduction of *SMN1* expression would not be relevant in vivo due to the fact that the *SMN1* gene is not functional at all in SMA patients. The data in

Figure 3 also shows the differences in luciferase inhibitory capacity of **1** and **2**. It can be seen that compound **1** was able to both increase the production of SMN protein (western) and inhibit luciferase. So without the creation of another cell line with a different reporter format, such as β-lactamase, GFP, or Renilla luciferase, it would be impossible to discriminate between SNM up-regulation and luciferase stabilization effects using our firefly luciferase reporter assay. In addition, the first triazine chemotype was found to have a very narrow

Scheme 3. Synthesis of the Piperidine Modification Analogues[a]
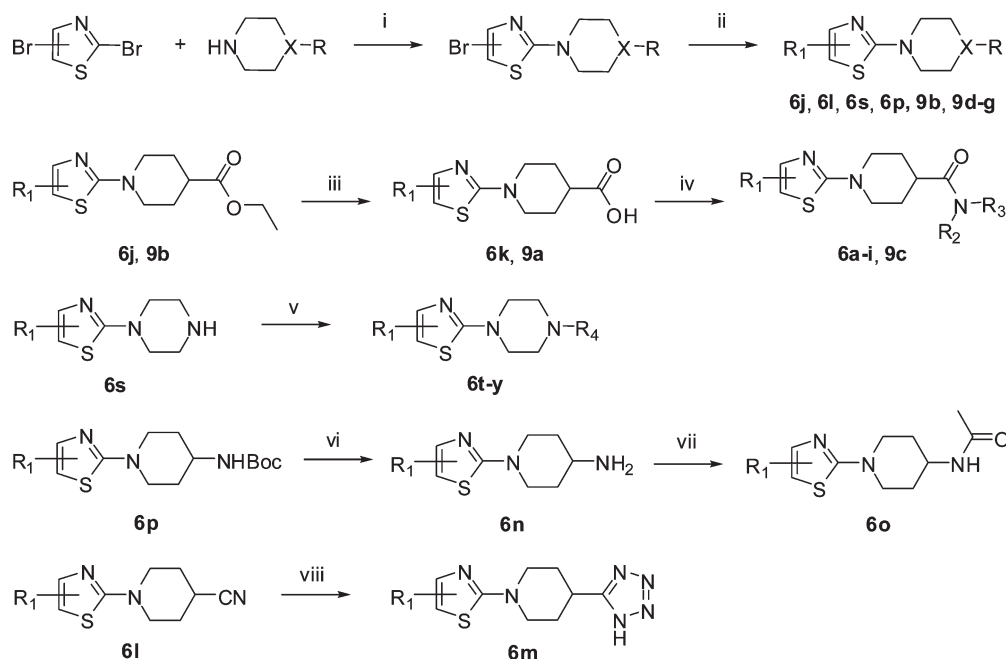
[a] Conditions and reagents: (i) triethylamine, μW; (ii) arylboronic acids or pinacol esters, 2.0 N Na$_2$CO$_3$, 5% Pd(PPh$_3$)$_4$, μW, 100 °C; (iii) LiOH, THF, H$_2$O; (iv) EDC, DMAP, μW, 100 °C; (v) KOCN, H$_2$O, or R$_5$COCl, triethylamine, or R$_6$SO$_2$Cl, triethylamine; (vi) trifluoroacetic acid; (vii) acetyl chloride, triethylamine; (viii) NaN$_3$, ZnBr$_2$, NaOH, dioxane, H$_2$O, 120 °C.

SAR. Therefore, we chose compound **2** as the prioritized series for further SAR optimization and biological evaluation because it possessed a more tractable SAR and drug-like properties. Furthermore, as reported in later section, this series displayed high cell permeability in Caco-2 cell permeability assay[40] and it had with no indication of being a glycoprotein (P-gp) substrate.[41]

Chemistry. Figure 4 shows the initial SAR strategy designed for the study of compound **2**, including evaluation of the nature and position of the aromatic substituents, the geometry and substituents at the thiazole core, as well as the modification of the piperidine functional group.
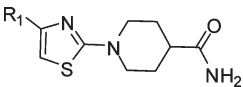
We developed convergent synthetic routes toward the original hit compound **2** and its 4-arylthiazolyl piperidine analogues (Scheme 1). Route (a) was designed to prepare analogues with the modification of the phenyl ring. Starting with 2,4-dibromothiazole, selective amination occurred at the 2-position of the thiazole ring to give the key building block 1-(4-bromothiazol-2-yl)piperidine-4-carboxamide.[42] Then, a mixture of an arylboronic acid or its corresponding pinacol ester and 1-(4-bromothiazol-2-yl)piperidine-4-carboxamide was irradiated under microwaves to induce a Suzuki type of cross-coupling reaction[43] using tetrakis(triphenylphosphine)palladium(0) as a catalyst to furnish the final 4-arylthiazolyl piperidine analogues. Alternatively, the route (b), a Suzuki coupling at the 4-position of the 2-methylthio-4-bromothiazole, followed by MCPBA oxidation of the methylthioyl group to the methylsulfonyl moiety, provided another building block 4-aryl-2-(methylsulfonyl)thiazole. However, the displacement of the methylsulfonyl group of the 4-aryl-2-(methylsulfonyl)thiazole with a secondary amine proved to be very difficult. Thus, all of the analogues described in this article were prepared through the amination–Suzuki coupling approach, route (a). This synthetic route was straightforward and provided for rapid SAR studies.
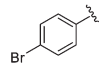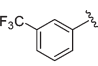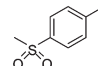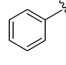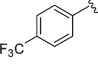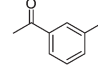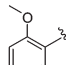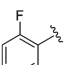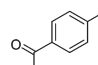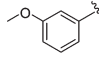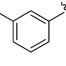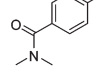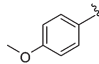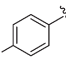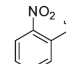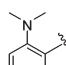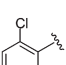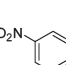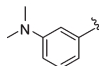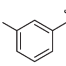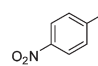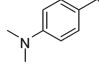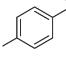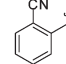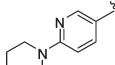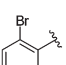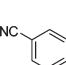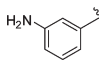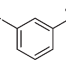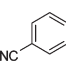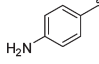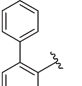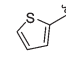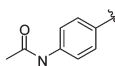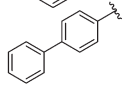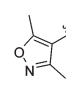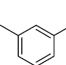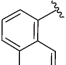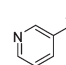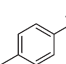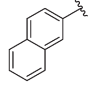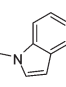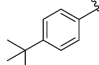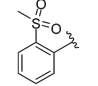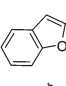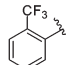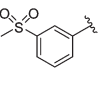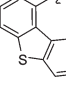
In a similar reaction fashion, if the starting material, 2,4-dibromothiazole is replaced by 2,5-dibromothiazole,[44] 2,5-dibromothiadiazole,[45] 5-bromo-2-chloropyrimidine,[46] 2,4-dichloropyrimidine,[47] 4,6-dichloropyrimidine,[48] or 2,4-dichloro-1,3,5-triazine,[49] the corresponding modifications at the thiazole core template can be accomplished as detailed in Scheme 2. It was also interesting to note that the replacement of thiazole with imidazole or *N*-methylimidazole was unsuccessful under the same reaction conditions. All aminated building blocks underwent the same type of Suzuki coupling procedure to give the desired final analogues.

Similar procedures were utilized to further explore modifications of the piperidine-4-carboxamide moiety (Scheme 3). In the process of typical amination–Suzuki steps, route (a), piperidine-4-carboxamide can be successfully switched to ethyl piperidine-4-carboxylate, piperazine, *tert*-butyl piperidin-4-ylcarbamate, piperidine-4-carbonitrile, 1-(piperidin-4-yl)ethanone as well as 4-(1*H*-imidazol-2-yl)piperidine, but not piperazine-1-carboxamide. Within our SAR studies, we were interested in examining several related substituted amide derivatives. Saponification of the ethyl ester afforded the appropriate acid, which can be readily coupled with amines to provide the final substituted amide modification analogues. We were also interested in replacing the piperidine with *N*-substituted piperazines. To access these derivatives, the free secondary amine of the piperazine ring can be easily converted into corresponding urea, amides, and sulfonylamides. Finally, a reverse amide bond analogue and a tetrazole analogue were successfully synthesized, as detailed in Scheme 3. Most of the final compounds were purified by preparative scale HPLC with reasonable yields.

SAR Discussion. Tables 1–7 disclose all of the analogues that were generated for this series to derive a SAR. The activity was reported showing two parameters: AC$_{50}$ (concentration

Table 1. SAR of 2,4-Substituted Thiazole Analogues Containing an Aromatic Substituent
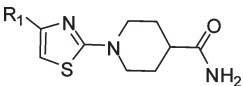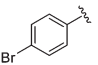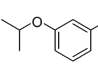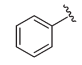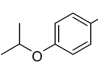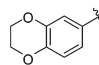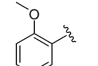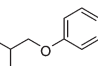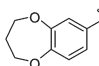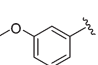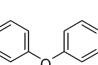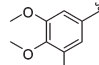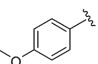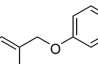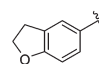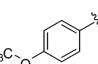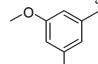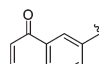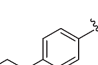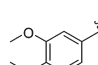
#	R_1	AC_{50} (μM)	ROI (%)	#	R_1	AC_{50} (μM)	ROI (%)	#	R_1	AC_{50} (μM)	ROI (%)
2		1.22	268	3p		387	100	4i		inactive	inactive
3a		7.72	167	3q		2.44	386	4j		3.87	356
3b		inactive	inactive	3r		2.44	274	4k		12.24	130
3c		1.94	357	3s		9.72	64	4l		12.24	51
3d		7.72	209	3t		3.87	288	4m		inactive	inactive
3e		inactive	inactive	3u		7.72	57	4n		3.87	20
3f		0.97	504	3v		12.24	53	4o		15.41	254
3g		30.74	64	3w		2.44	381	4p		inactive	inactive
3h		6.13	100	4a		inactive	inactive	4q		inactive	inactive
3i		inactive	inactive	4b		30.75	57	4r		9.72	49
3j		inactive	inactive	4c		inactive	inactive	4s		7.72	51
3k		inactive	inactive	4d		24.42	58	4t		inactive	inactive
3l		30.74	187	4e		inactive	inactive	4u		inactive	inactive
3m		1.22	439	4f		7.72	162	4v		7.72	534
3n		3.87	243	4g		inactive	inactive	4w		15.41	100
3o		inactive	inactive	4h		inactive	inactive	4x		30.74	369

necessary to reach 50% of maximum luciferase signal) and rate of induction (ROI) (efficacy indicated as maximum percentage of

luciferase signal with respect to basal levels), which were used to conduct SAR analysis. Both parameters, ROI and AC_{50}, were

Table 2. SAR of 2,4-Substituted Thiazole Analogues Containing a Phenoxy Substituent

#	R_1	AC_{50} (μM)	ROI (%)	#	R_1	AC_{50} (μM)	ROI (%)	#	R_1	AC_{50} (μM)	ROI (%)
2	4-bromophenyl	1.22	268	5c	3-isopropoxyphenyl	0.77	605	5j	benzo[1,3]dioxole	2.44	359
3a	phenyl	7.72	167	5d	4-isopropoxyphenyl	3.87	178	5k	2,3-dihydrobenzo[1,4]dioxine	0.77	459
3b	2-methoxyphenyl	inactive	inactive	5e	4-isobutoxyphenyl	3.07	54	5l	benzo[1,4]dioxepine	0.49	443
3c	3-methoxyphenyl	1.94	357	5f	4-phenoxyphenyl	4.87	240	5m	3,4,5-trimethoxyphenyl	19.40	73
3d	4-methoxyphenyl	7.72	209	5g	4-benzyloxyphenyl	Inactive	Inactive	5n	2,3-dihydrobenzofuran	12.24	401
5a	4-trifluoromethoxyphenyl	3.07	297	5h	3,5-dimethoxyphenyl	7.72	45	5o	chromone	15.41	589
5b	4-ethoxyphenyl	3.87	212	5i	3,4-dimethoxyphenyl	12.24	59				

evaluated and optimized, as the ideal compound should provide maximum SMN protein production with minimal concentration of a given compound.

The hit compound **2** identified from the primary screen was resynthesized and found to possess an AC_{50} value of 1.22 μM with a ROI of 268%. Our early efforts were focused on improving both parameters in order to further explore the SAR for this chemotype. To conduct a comprehensive SAR (Table 1) for the aromatic group at the 4-position of the thiazole ring while exploring the steric and electronic effects of the substituents, the thiazole and piperidine rings were held constant, as shown in Table 1. We first examined the effect of the substituent position at the phenyl ring on potency (AC_{50}) and efficacy (ROI). With the exception of the *ortho*-fluoro substituted analogue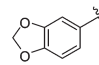 **3r** (AC_{50} = 2.44 μM, ROI = 274%), all other *ortho*-substituents were either inactive (**3b**, **3e**, **3o**, **4a**, **4c**, **4e**, **4g**, **4m**, and **4p**) or were significant less active (**3u** and **4x**) versus compound **2**. These data indicated the potential necessity of having a coplanar conformation between the two aromatic rings to maintain good activity. In contrast to *ortho*-substitutions, substituents at *meta* or *para* positions were generally well tolerated. Regarding the electronic nature of the substituents, an electron-donating functional group at the *meta* or *para* position tended to provide better activity and efficacy than the corresponding electron-withdrawing group (**3c**, **3f** vs **4h**, **4n**, **4q** and **3d** vs **4i**, **4o**, **4r**). In addition, halo, methyl, or trifluoromethyl substitutions at *para* and *meta* position were also tolerated. Several substituents slightly increased or maintained the activity compared to the efficacy of the hit compound **2**, such as the *meta*-methoxy substituted analogue **3c** (AC_{50} = 1.94 μM,

ROI = 357%), *meta*-N,N-dimethylamino substituted analogue **3f** (AC_{50} = 0.97 μM, ROI = 504%), and *para*-methyl substituted analogue **3m** (AC_{50} = 1.22 μM, ROI = 439%). Regarding heteroaromatic ring substitutents, none of analogues **4s**−**4u** had a positive impact on either parameter compared to the parent compound **2**. We also studied several polycyclic aromatic ring analogues (**4e**, **4f**, and **4v**−**4x**). However, most had either no activity or decreased activity and efficacy.

Given the improved potency and efficacy observed with the electron-donating substituents, we chose to screen a large number of phenoxy substitutents (Table 2). Several additional electron-donating substituents were tolerated including *meta*-isopropoxyphenyl (**5c**, AC_{50} = 0.77 μM, ROI = 605%). We also examined the 3,5- or 3,4-disubstituted analogues (**5h** and **5i**, AC_{50} = 7.72 and 12.24 μM, ROI = 45% and 59%, respectively) and 3,4,5-trisubstituted derivative (**5m**, AC_{50} = 19.4 μM, ROI = 73%). Surprisingly, these modifications resulted in a huge loss of both activity and efficacy. Interestingly, this loss could be regained by bridging two substituents together. Furthermore, the resulting cyclic poly phenolic-ethers demonstrated a clear trend of improvement in activity in line with ring size (5 < 6 < 7, **5j**, **5k**, **5l**, AC_{50} = 2.44, 0.77, and 0.49 μM, respectively).

With several improved analogues in hand (analogues **5c**, **5k**, and **5l**), we further studied the SAR of the piperidine ring moiety as shown in Table 3. In general, mono- or disubstituted amide derivatives **6a**−**6i** had worse potency and efficacy, with the exception of the phenylamide derivative (**6e**, AC_{50} = 2.44 μM, ROI = 262%), which was about the same as the hit compound **2**. It is also important to remark that both the carboxylic acid **6k** and

Table 3. SAR of 2,4-Substituted Thiazole Analogues with Modifications of the Primary Amide Moiety and Piperidine Ring

#	R_1	AC_{50} (μM)	ROI (%)	#	R_1	AC_{50} (μM)	ROI (%)	#	R_1	AC_{50} (μM)	ROI (%)
2		1.22	268	6i		inactive	inactive	6q		19.40	272
6a		7.72	101	6j		7.72	550	6r		inactive	inactive
6b		30.75	43	6k		4.87	554	6s		24.42	-97
6c		30.75	77	6l		30.74	78	6t		3.07	234
6d		inactive	inactive	6m		12.24	67	6u		12.24	89
6e		2.44	262	6n		2.44	182	6v		inactive	inactive
6f		inactive	inactive	6o		15.41	-57	6w		inactive	inactive
6g		6.13	32	6p		inactive	inactive	6x		inactive	inactive
6h		inactive	inactive					6y		inactive	inactive

the corresponding ethyl ester **6j** derivatives were about 4- and 6-fold less active, respectively, compared to compound **2**, while both showed improved efficacy (**6k**, AC_{50} = 4.87 μM, ROI = 554%, and **6j**, AC_{50} = 7.72 μM, ROI = 550%, respectively). This result indicated that only the carbonyl functional group might be involved in a potential hydrogen bond interaction. This was further supported by significant loss of potency of the noncarbonyl bearing analogues **6q**−**6s**. When the amide moiety was replaced by cyano or tetrazole groups, the resulting derivatives (analogues **6l** and **6m**) also showed a loss of potency. Reverse amide **6o** and carbamate **6p** analogues were not tolerated either. Surprisingly, a free amine moiety seemed to be tolerated (**6n**, AC_{50} = 2.44 μM, ROI = 182%). In contrast to the modification of the amide moiety, the piperidine ring was found to be necessary to maintain potency. Interestingly, a piperazine analogue **6t**, which represents another retro-amide variation, displayed reasonable good activity. In contrast, all of the other piperazine derivatives, **6u**−**6y**, were essentially inactive.

In general, replacement of the 2,4-disubstituted thiazole ring with a 2,4-disubstituted pyrimidine maintained or improved potency and efficacy (Table 4). Placement of the piperidine-4-carboxamide

substituent between the two heteroaromatic nitrogen atoms and aromatic substituent at the 4-position increased the potency of the molecule by 2−3-fold (**7d**, AC_{50} = 0.387 μM, ROI = 387%, and **7i**, AC_{50} = 0.772 μM, ROI = 446%). The aromatic substituent at the 5 position of the pyrimidine was also tolerated as represented by analogue **7b** (AC_{50} = 0.613 μM, ROI = 236%), although its efficacy was only half in comparison with the above-described pyrimidine analogues. The *meta*-isopropoxyphenyl substituted derivative **7g** was found to be the best analogue in this series, with about 9-fold increase in potency (**7g**, AC_{50} = 0.154 μM, ROI = 298%) versus the hit compound **2**. Derivatives bearing a monofluoro substituent at 5 position of the pyrimidine gave an additional 2−4-fold improvement in potency (**7j** vs **7i** and **7l** vs **7n**). Replacement of the pyrimidine for 1,3,5-triazine resulted in analogues with decreased potency (**7i** vs **7k** and **7h** vs **7p**). These results indicated that the potency of these compounds would not be improved by the introduction of additional nitrogens in the pyrimidine core ring. An *ortho*-methyl substituted pyrimidine derivative **7o** was found to be totally inactive, which further supported an earlier observation for requirement of a coplanar conformation for this portion of the molecule for activity. On the other hand, when the pyrimidine substitution patterns were reversed,

Table 4. SAR of Analogues with Modifications of Thiazole Core

#	Structure	AC_{50} (μM)	ROI (%)	#	Structure	AC_{50} (μM)	ROI (%)
7a		inactive	inactive	7j		0.387	373
7b		0.613	236	7k		1.22	200
7c		inactive	inactive	7l		3.07	141
7d		0.387	387	7m		3.87	81
7e		0.387	444	7n		12.24	306
7f		1.22	364	7o		inactive	inactive
7g		0.154	298	7p		2.44	186
7h		1.54	234	7q		7.72	211
7i		0.772	446				

with the aromatic substituent between the two heteroaromatic nitrogen atoms and the piperidine-4-carboxamide substituent at the position 4, the resulting derivatives decreased activity by 8—16-fold (7i vs 7n and 7j vs 7l). In addition, moving two nitrogen atoms around the pyrimidine also decreased the potency by 5-fold (7i vs 7m and 7h vs 7q). These findings lead to the hypothesis that the sterically accessible nitrogen atom adjacent to the piperidine group is involved in a hydrogen bond interaction, serving as a hydrogen bond acceptor.

Table 5 shows modifications for the thiazole portion of the molecule. Switching the aromatic substituent from the 4 position to 5 position of the thiazole core ring increased the potency by 5-fold and efficacy by 2-fold (8g, AC_{50} = 0.224 μM, ROI = 599%). We speculated that this increment was due to accessibility of the thiazole nitrogen for involvement in hydrogen bond interactions with the putative molecular target. Replacement of a CH with a N atom in the thiazole core resulting in 1,3,4-thiadiazole led to a 3—10-fold loss of potency (8a vs 8b; 8c vs 8d; 8e vs 8f; and 8g vs 8h). These results are analogous to replacement of the pyrimidine with the triazine and are due to the electronic effect of the core ring.

With the rationale that the SAR of the aromatic substituents from the 2,4-substituted thiazole could be translated to a 2,5-substituted thiazole series, the SAR of the different electron-donating groups on the phenyl moiety was explored (Table 5 and Table 6). Gratifyingly, several electron-donating groups on the phenyl ring indeed produced a synergistic effects on both potency and efficacy (8a, AC_{50} = 0.038 μM, ROI = 370%; 8e, AC_{50} = 0.039 μM, ROI = 550%; 8l, AC_{50} = 0.077 μM, ROI = 709%; 8m, AC_{50} = 0.031 μM, ROI = 576%). Again, the 3,4-disubstituted derivative 8n again was less active than the corresponding ring closed analogues 8a and 8o—8q. Several cyclic meta-N,N-disubstituted aminophenyl derivatives, 8r—8t, were examined and were found to be less active than the parent meta-N,N-dimethylaminophenyl derivative 8e.

The modification of the amide moiety in the 2,5-substituted thiazole system was further explored, as shown in Table 7. For these studies, 3,4-dihydro-2H-benzo[b][1,4]dioxepin-7-yl or meta-N,N-dimethylaminophenyl were chosen as the two aromatic substituents at the C5 position of thiazole core ring. The results demonstrated that the replacement of amide with an acid

Table 5. SAR of Analogues Having 2,5-Substituted Thiazole and Thiadiazole Cores

#	Structure	AC$_{50}$ (µM)	ROI (%)
8a		0.038	370
8b		0.122	257
8c		0.077	609
8d		0.244	54
8e		0.039	550
8f		0.387	448
8g		0.244	599
8h		inactive	inactive
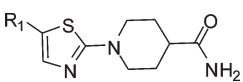
had a clear advantage for potency with a 3-fold improvement, but with a slight loss of efficacy (**9a** with best AC$_{50}$ = 0.012 µM, ROI = 325%). Ethyl ester or phenylamide derivatives were also tolerated (**9b**, AC$_{50}$ = 0.031 µM, ROI = 320%, and **9c**, AC$_{50}$ = 0.049 µM, ROI = 353%). However, the imidazole and methylketone replacements were not tolerated (**9d**, **9e**, **9f**, and **9g**).
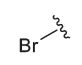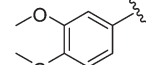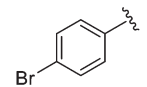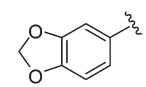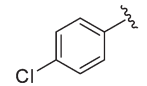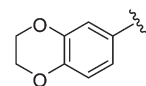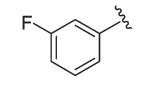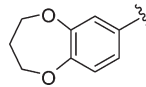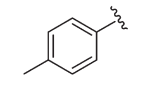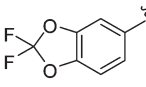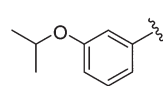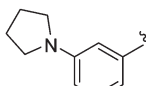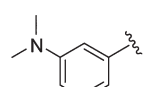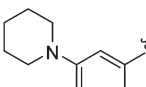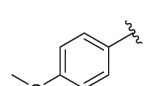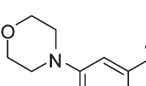
Secondary Validation Assays. With the SAR assessment established for this series, a number of selected analogues featuring desirable potency below 150 nM in the reporter assay were then examined to evaluate the effect on the human SMN protein expression using fibroblasts from SMA patients. We incubated a fibroblast cell line from a type I SMA patient (3813 cell line) with different doses of analogues and assessed the SMN protein level by quantitative Western blotting (Figure 5). We observed that analogue **8m** at 37 nM increased the SMN protein level by 2–3-fold. The SMN protein level was decreased with increasing drug concentration. This result matched with the bell-shaped dose–response curve observed in the *SMN2*-luciferase reporter assay. This could be due to decreased compound solubility at higher concentrations or it may reflect the intrinsic mechanism of action. Analogue **9a** showed a dose-dependent trend between 37 nM to and 1 µM concentration.

Other selected agents (**9c**, **8c**, and **8l**) all showed an up-regulation of SMN protein at concentrations ranging between 37 and 333 nM.

Furthermore, the increase in SMN protein production led us to explore whether the arylpiperidine analogues had an effect on the overall number of SMN positive foci or gems in the nucleus. This would corroborate that the increased protein amounts represent functional SMN protein. SMN protein is predominately a cytoplasmic protein, but in the nucleus, SMN localizes to distinct punctuate bodies, often referred to as gems (gemini of coiled [Cajal] bodies). There is a direct correlation between the number of gems and total SMN protein production in the cell.[50] Gem counts are commonly used as another metric to score the amount of total SMN protein expressed on a cell-to-cell basis. The number of nuclei with gems and the number of gems per cell were both significantly reduced in type I SMA cells. Only 3.3% of nuclei have gems in fibroblast cells from SMA type I patients (cell line 3813), while 24.8% of nuclei have gems in fibroblast from a carrier parent (3814 cell line). We treated human type I SMA fibroblasts with increasing concentrations (37–3000 nM) of arylpiperidine analogues **8a**, **8m**, and **9a** for 3 days, and the number of gems per 100 nuclei were examined (Figure 6). Analogue **8m** treatment yielded more than a 2-fold of increase

Table 6. SAR of 2,5-Substituted Thiazole Analogues Containing an Aromatic Substituent

#	R$_1$	AC$_{50}$ (μM)	ROI (%)	#	R$_1$	AC$_{50}$ (μM)	ROI (%)
8i	Br	inactive	inactive	8n	(3,4-dimethoxyphenyl)	9.72	209
8g	(4-bromophenyl)	0.244	599	8o	(benzodioxole)	0.049	590
8j	(4-chlorophenyl)	0.154	498	8p	(benzodioxane)	0.097	424
8k	(3-fluorophenyl)	2.44	601	8a	(benzodioxepine)	0.038	370
8c	(4-methylphenyl)	0.077	609	8q	(difluorobenzodioxole)	0.194	598
8l	(3-isopropoxyphenyl)	0.077	709	8r	(3-pyrrolidinophenyl)	0.387	685
8e	(3-dimethylaminophenyl)	0.039	550	8s	(3-piperidinophenyl)	1.54	565
8m	(4-methylthiophenyl)	0.031	576	8t	(3-morpholinophenyl)	2.44	275
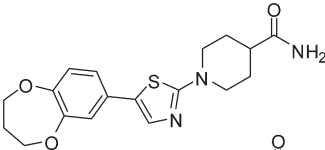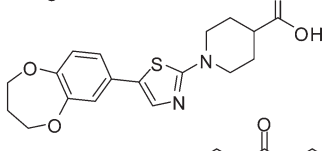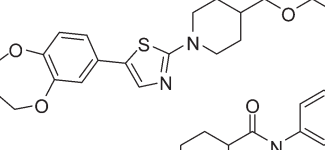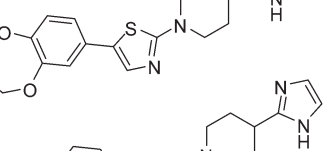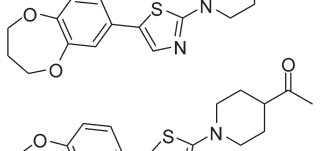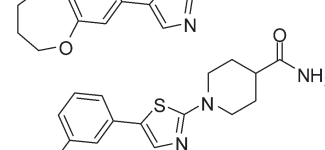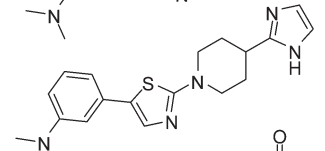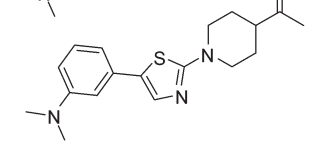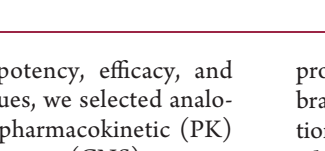
of the number of the gems at the low 37 nM dose. With increasing concentration, the number of gems was reduced, which agreed with the previous findings on our reporter and westerns experiments. Analogue **9a** also showed an 80% increase of the gem numbers at 37–1000 nM concentrations and aslightly decrease at 3000 nM. However, analogue **8a** did not show any activity in this assay.

Mechanism of Action. Compounds were initially characterized using RT-PCR to measure RNA expression levels and exon 7 inclusion within our reporter cell line (not endogenous SMN). Some analogues (**2**, **3f**, and **8e**) showed a slight increase in total SMN-luciferase transcripts, but there was almost no increase in exon 7 mRNA (data not shown). Therefore, the mechanism of action of our series is likely post-transcriptional, in contrast to the HDAC and DcpS inhibitors previously identified. Perhaps this mechanism includes increasing the stability of the SMN protein and/or affecting its degradation, but it is distinct from D156844, a deCode compound,[29a] which had no activity in the present screening assay. So far, no other SMN modulator has been described as having this type of activity, and therefore it will be interesting for the scientific community to have a better understanding of its properties, mechanism, and potential pharmaceutical application. The

SMNΔ7 protein, the primary product from *SMN2*, is functional in the context of low levels of exon-7 included SMN protein but it is proteolytically unstable. It will be interesting to explore whether the present series has an impact on the stability of the SMNΔ7 derived truncated SMN protein, thereby establishing a new paradigm for the treatment of SMA.

ADME Properties and Pharmacokinetics. In addition, several of the most potent analogues were profiled for mouse liver microsomal stability and cell permeability in Caco-2 cells (Table 8). For the microsomal stability tests, we decided to evaluate the amount of parent compound remaining following incubation at three different time periods: 10, 15, and 60 min. This allowed us to both calculate both intrinsic clearance and model half-lives. The original hit compound **2** was found to have a relatively short half-life (12 min). Analogues **8c**, **8m**, and **9c** all had a very short half-lives <10 min. Analogues **8b**, **8l**, and **9a** had half-lives of more than 30 min. In the bidirectional Caco-2 cell permeability assay, analogues **7g**, **8b**, and **9a** were found to exhibit high permeability, while analogues **8b** and **9a** had efflux ratios of 2.4 and 1.3 respectively and analogue **8l** had a promising efflux ratio of 0.05. The cell permeability of analogue **8m** was not great, although the efflux ratio was acceptable (0.125).

Table 7. SAR of 2,5-Substituted Thiazole Analogues with Modifications of the Primary Amide

#	Structure	AC$_{50}$ (μM)	ROI (%)
8a		0.038	370
9a		0.012	325
9b		0.031	320
9c		0.049	353
9d		2.44	129
9e		inactive	inactive
8e		0.039	550
9f		7.72	188
9g		3.07	224

In consideration of a balance of potency, efficacy, and ADME properties of all current analogues, we selected analogues **8l** and **9a** for full mouse in vivo pharmacokinetic (PK) studies to evaluate the central nervous system (CNS) penetration of this series (Table 9). The plasma and brain concentration of analogues **8l** and **9a** in male Swiss Albino mice after a single oral gavage administration at a dose of 30 mg/kg were measured. As shown in Table 9, the brain to plasma ratio of analogues **8l** and **9a** in male Swiss Albino mice was found to be 0.29 and 0.028, respectively. Both analogues **8l** and **9a** possessed a reasonable long half-life in brain ($t_{1/2}$ = 5.44 and 13.69 h) as well as in plasma ($t_{1/2}$ = 5.78 and 11.18 h). The concentration of analogue **8l** in brain reached at 1.28 μmol/kg (C_{max}) in only 5 min, and a concentration above its AC$_{50}$ of 0.077 μM was maintained for more than 4 h. Despite its high plasma

protein binging (94.9%) for analogue **9a**, its concentration in brain reached 1.23 μmol/kg (C_{max}) in 15 min and a concentration above AC$_{50}$ concentration of 0.012 μM for over 24 h. In addition, no behavioral disturbance was observed in animals administered with both tested compounds throughout the whole study period. Oral administration with good brain exposure will be preferred for demonstrating in vivo activity, as many of the current animal models require chronic administration of the drug.

■ CONCLUSION

In summary, after several rounds of medicinal chemistry SAR studies, we were able to improve the potency of the hit compound by ~100-fold from μM to low double-digit nM in
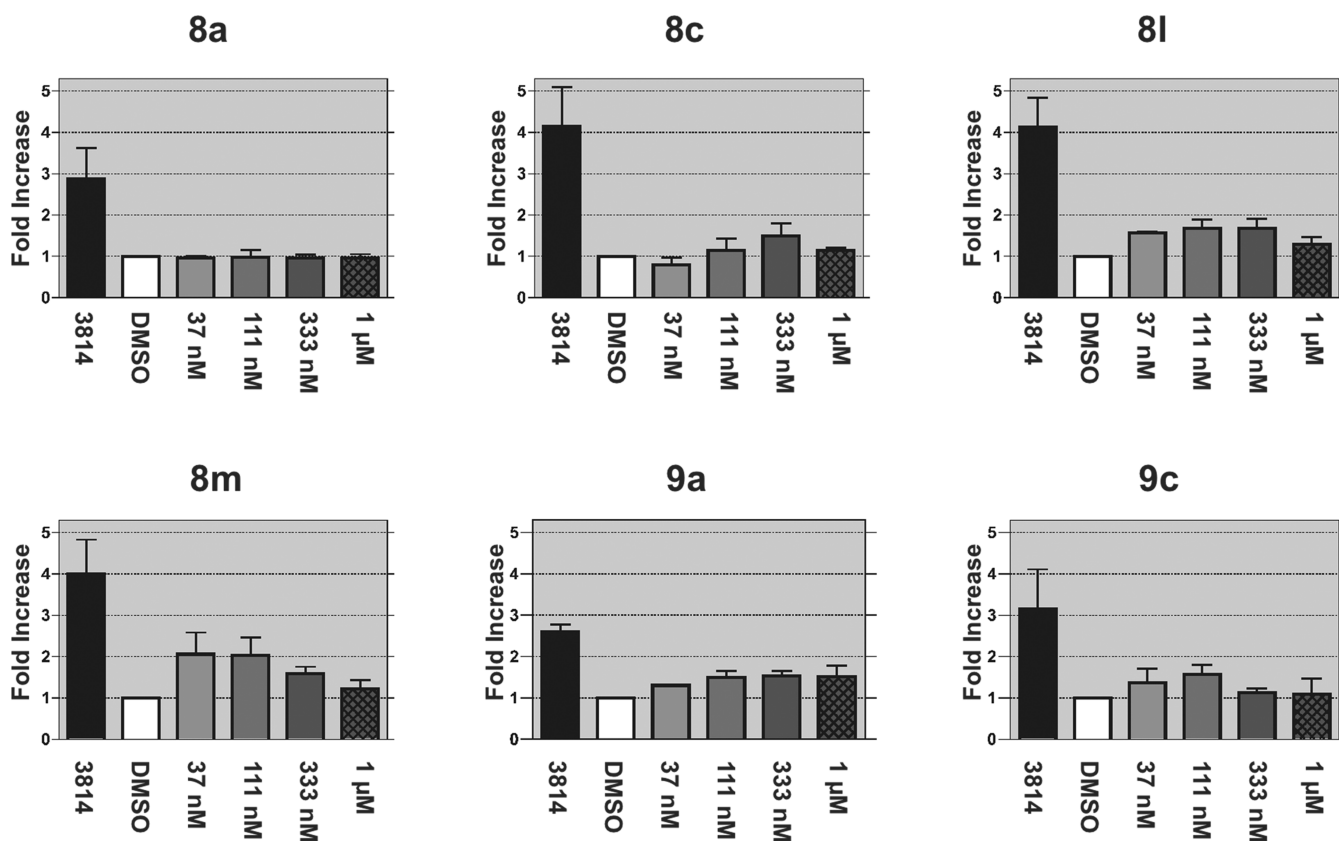
Figure 5. Quantification by Western blot of SMN levels after treatment with drug compounds at different concentrations, as indicated.
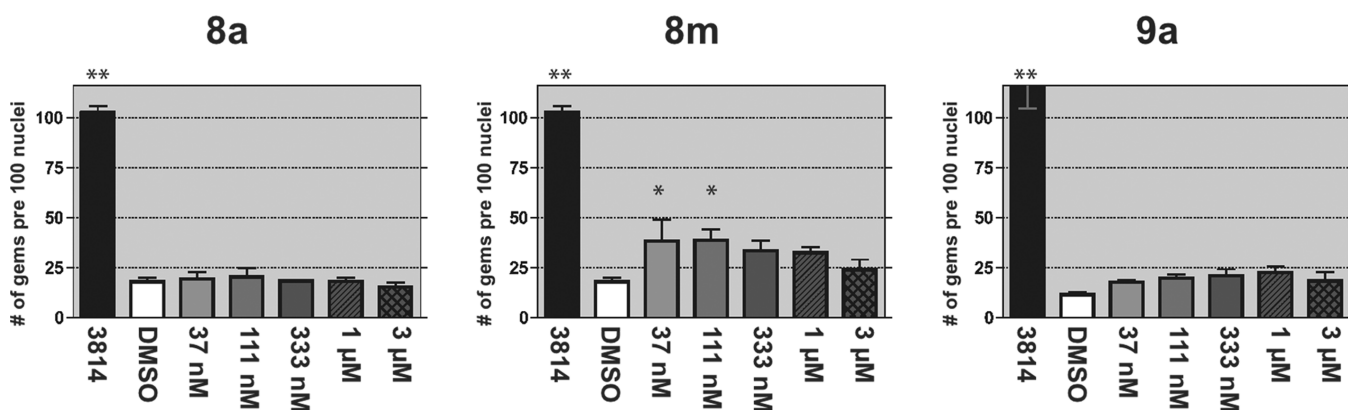
Figure 6. Number of gems per 100 nuclei after treatment with drug compounds at different concentrations, as indicated.

our cell-based *SMN2*-luciferase reporter assay, we were also able to increase the rate of SMN protein production 3–7-fold. From this study, analogues **8a** (AC_{50} = 0.038 μM, ROI = 370%), **8e** (AC_{50} = 0.039 μM, ROI = 550%), **8l** (AC_{50} = 0.077 μM, ROI = 709%), **8m** (AC_{50} = 0.031 μM, ROI = 576%), and **9a** (AC_{50} = 0.012 μM, ROI = 325%) were identified as novel SMN protein modulators. In the field, it is generally believed that an up-regulation of SNM production of at least 20% above patient basal levels will be necessary to have a therapeutic impact. Our best molecules clearly surpass that mark, in vitro, increasing levels of SMN protein between 100% and 300% at low nanomolar concentrations when they were tested in our primary reporter assay, as well as in relevant orthogonal assays such as Western blot and gems assays with patient fibroblasts. In consideration of all the aspects including ADME properties, analogues **8l** and **9a** possessed the best combination of potency, efficacy, mouse liver microsomal stability, and cell permeability of all the analogues presented in this study. Moreover, analogues **8l** and **9a** showed good oral absorption and CNS penetration upon oral gavage administration at a reasonable dose of 30 mg/kg, providing levels of exposure above their AC_{50} for more than 4 h in brain with no sign of toxicity or behavior disturbance in animals.

Table 8. Selected ADME Properties Assessment for Chosen Lead Compounds[a]

no.	SMN2 AC_{50} (fiM)	ROI (%)	luciferase inh. IC_{50} (μM)	mouse liver microsome $T_{1/2}$ (min)	Caco-2 permeability mean P_{app} A $\rightarrow$ B (10^{-6} cm s^{-1})	Caco-2 permeability mean P_{app} B $\rightarrow$ A (10^{-6} cm s^{-1})
2	1.22	268	inactive	12	30.7	12.1
6k	4.87	554	1.60	ND	32.6	12.0
7g	0.154	298	10	18	40.1	17.3
8a	0.038	370	3.2	30	13.1	9.9
8b	0.122	257	3.2	>60	21.2	51.2
8c	0.077	609	6.4	7	ND	ND
8l	0.077	709	0.80	30	6.1	0.3
8m	0.031	576	40	2	1.6	0.2
9a	0.012	325	0.005	>60	33.8	44.1
9c	0.049	353	4.0	<15	ND	ND

[a] Microsomal stability analysis was performed by Cerep and was based upon duplicate incubations of test reagent with mouse liver microsomes at 37 °C as described (www.cerep.com). LC/MS/MS was utilized to quantitate remaining test compound. Test compounds were applied at standard concentrations (1 μM). Caco-2 permeability analysis was performed by Cerep as described (www.cerep.com). Data are expressed in P_{app} (apparent permeability) in 10^{-6} cm s^{-1}. Colchicine and ranitidine were used as a low permeability controls (colchicine: mean A$\rightarrow$B < 0.1 and mean B$\rightarrow$A = 7.9; ranitidine mean A$\rightarrow$B = 0.2 and mean B$\rightarrow$A = 2.8), propranolol was used as a high permeability control (mean A$\rightarrow$B = 41.0 and mean B$\rightarrow$A = 39.4), and labetalol was used as a P-gp substrate control (mean A$\rightarrow$B = 7.3 and mean B$\rightarrow$A = 36.6). Test compounds were applied at standard concentrations (10 μM).

■ EXPERIMENTAL SECTION

Biology Reagents. All cell culture reagents were purchased from Invitrogen. The white solid-bottom, 1536-well, tissue culture treated plates came from Greiner. The OneGlo luciferase detection reagent was from Promega. The luciferase enzyme and buffers came from Sigma Aldrich. The 4f11 and 4B7 SMN antibodies were provided to EJA as a generous gift from Christian Lorson (University of Missouri). Goat antimouse HRP-conjugated secondary and α-tubulin antibodies (DM1α) were supplied by Sigma.

Luciferase Reporter Assay. HEK-293 cells stably expressing the SMN1 or SMN2 reporter construct were maintained and passaged in complete DMEM media containing phenol red, glutamax, sodium pyruvate, 10% FCS, 1× pen/strep, and 200 μg/mL hygromycin. Cells were assayed in the same media lacking only hygromycin. For the HTS, cells were plated at a density of 2000 cells/well in 5 μL of media and were allowed to adhere overnight at 37 °C in 90% humidity with 5% CO_2. After incubation, cells received 23 nL of compound library (in 100% DMSO) by pintool addition (Kalypsys). The final concentration of DMSO was 0.46%. The screen was conducted in a 7-point qHTS titration with a final concentration of 50 μM to 25 nM. The positive control compound used was sodium butyrate (4.5 mM final concentration) and the negative control compound was DMSO. Plates were incubated in the presence of compounds for 30−36 h in the humidified incubator. After incubation, cells were treated with 3 μL of OneGlo luciferase detection reagent and incubated at room temperature for 5−15 min. Luminescence was detected on a Viewlux CCD based instrument (Perkin-Elmer) with settings of 60 s integration and high speed 2× binning. Data were normalized against sodium butyrate (100%) and DMSO (0%) treatments.

Firefly Luciferase Enzyme Assay. The firefly luciferase enzyme was assayed at 5 nM in buffer consisting of 50 mM Tris-acetate pH 7.6, 10 mM mg acetate 0.05% BSA, 0.01% Tween. Enzyme (2.5 μL/well) was dispensed in a white solid-bottom 1536-well plate, and compounds (23 nL) were added using a pintool. Plates were incubated at room temperature for 5 min, followed by the addition of 2.5 μL of OneGlo luciferase detection reagent. Luminescence was detected in the Viewlux with a 1 s integration time, no binning, and medium camera sensitivity.

SMN Protein Detection. For detection of SMN protein in patient fibroblasts, 8000 cells per cm^2 were plated 24 h prior to drug addition. Fresh media and compound were added every 24 h. After 72 h of

incubation, cells were harvested, washed with cold PBS, and lysed as above. We have determined that 10 μg total protein per lane is within the linear range for immunoblot detection of SMN and α-tubulin. Western blots were probed for SMN with the 4f11 mouse monoclonal antibody and α-tubulin. Quantification of protein was performed with Fujifilm LAS-4000 multifunctional imaging System. The signal intensity was measured for each band on an immunoblot, normalized to the loading control, and the fold increase was determined in relation to the appropriate DMSO treated control.

Chemistry General Methods. All solvents were of anhydrous quality, purchased from Aldrich Chemical Co., and used as received. Commercially available starting materials and reagents were purchased from Aldrich, TCI, and Acros and were used as received. Analytical thin layer chromatography (TLC) was performed with Sigma Aldrich TLC plates (5 cm × 20 cm, 60 Å, 250 μm). Visualization was accomplished by irradiation under a 254 nm UV lamp. Chromatography on silica gel was performed using forced flow (liquid) of the indicated solvent system on Biotage KPSil prepacked cartridges and using the Biotage SP-1 automated chromatography system. ^{1}H NMR spectra were recorded on a Varian Inova 400 MHz spectrometer. Chemical shifts are reported in ppm with the solvent resonance as the internal standard (CDCl$_3$ 7.27 ppm, DMSO-d_6 2.49 ppm, for ^{1}H NMR). Data are reported as follows: chemical shift, multiplicity (s = singlet, d = doublet, t = triplet, q = quartet, sep = septet, quin = quintet, br = broad, m = multiplet), coupling constants, and number of protons. Low resolution mass spectra (electrospray ionization) were acquired on an Agilent Technologies 6130 quadrupole spectrometer coupled to an Agilent Technologies 1200 series HPLC. The HPLC retention time were recorded through standard gradient 4% to 100% acetonitrile (0.05% TFA) over 7 min using Luna C$_{18}$ (3 μm, 3 mm × 75 mm) column with a flow rate of 0.800 mL/min. High resolution mass spectral data were collected in-house using an Agilent 6210 time-of-flight mass spectrometer coupled to an Agilent Technologies 1200 series HPLC system. If needed, products were purified via a Waters preparative HPLC equipped with a Phenomenex Luna or Gemini C$_{18}$ reverse phase (5 μm, 30 mm × 75 mm) column having a flow rate of 45 mL/min. The mobile phase was a mixture of acetonitrile (0.1% TFA) and H$_2$O (0.1% TFA) for acidic conditions and a mixture of acetonitrile and H$_2$O (0.1% NH$_4$OH) for basic conditions. Samples were analyzed for purity on an Agilent 1200 series LC/MS equipped with a Luna C$_{18}$ reverse phase (3 μm,

Table 9. Pharmacokinetic Data for Analogues 8l and 9a Following Oral Gavage Administration Dosing to Mice

oral administration of 30 mg/kg of **8l** in male Swiss Albino mice				
mean plasma concentration			mean brain concentration	
sampling time (h)	mean (ng/mL)	mean (μM)	mean (ng/g)	mean (μmol/kg)
0	0	0	0	0
0.083	1286	3.72	444	1.28
0.25	416	1.2	109	0.31
0.5	416	1.2	138	0.4
1	439	1.27	207	0.6
2	206	0.6	85	0.23
4	0.98	0.0028	29	0.083
8	8.49	0.025	0	0
12	6.71	0.019	0	0
24	20.64	0.06	7.78	0.023
PK parameters	unit	estimate	PK parameters	unit	estimate
T_{max}	h	0.083	T_{max}	h	0.083
C_{max}	μM	3.72	C_{max}	μmol/kg	1.28
$T_{1/2}$	h	5.78	$T_{1/2}$	h	5.44
$AUC_{plasma}(AUC_{last})$	h·ng/mL	1857	$AUC_{plasma}(AUC_{last})$	h·ng/mL	546
AUC_{INF}	h·ng/mL	1429	AUC_{INF}	h·ng/mL	607
AUC_{brain}/AUC_{plasma}	%	29			

oral administration of 30 mg/kg of **9a** in male Swiss Albino mice					
mean plasma concentration				mean brain concentration	
sampling time (h)	mean (ng/mL)	mean (μM)	free concentration (μM)[a]	mean (ng/g)	mean (μmol/kg)
0	0	0	0	0	0
0.083	15990	44.4	2.26	173	0.48
0.25	15038	41.7	2.13	442	1.23
0.5	14822	41.1	2.1	409	1.14
1	7575	21	1.07	214	0.59
2	5990	16.6	0.85	157	0.43
4	3890	10.8	0.55	129	0.36
8	4537	12.6	0.64	114	0.32
12	1645	4.57	0.23	47	0.13
24	1570	4.36	0.22	48	0.13
PK parameters	unit	estimate	PK parameters	unit	estimate	
T_{max}	h	0.083	T_{max}	h	0.25	
C_{max}	μM	44.4	C_{max}	μmol/kg	1.23	
$T_{1/2}$	h	11.18	$T_{1/2}$	h	13.69	
$AUC_{plasma}(AUC_{last})$	h·ng/mL	77768	$AUC_{plasma}(AUC_{last})$	h·ng/mL	2167	
AUC_{INF}	h·ng/mL	103094	AUC_{INF}	h·ng/mL	3115	
AUC_{brain}/AUC_{plasma}	%	2.8				

[a] Based on 94.9% of plasma protein binding for **9a**

3 mm × 75 mm) column having a flow rate of 0.800 mL/min over a 7.0 min gradient and a run time of 8.5 min. Purity of final compounds was determined to be >95%, using a 3 μL injection with quantitation by AUC at 220 and 254 nm (Agilent diode array detector).

General Protocol A. A mixture of bromo- or chlorosubstituted building block (0.100 mmol), boronic acid or pinacol ester (0.200 mmol), and tetrakis(triphenylphosphine)palladium (5.00 μmol) in DMF (1.50 mL) or CH_3CN (1.50 mL), and 2.0 M Na_2CO_3 aqueous

solution (0.50 mL) was heated in a microwave at 100 °C for 30 min. The reaction mixture was cooled to room temperature and treated with a small portion of Si-THIOL to get rid of palladium. The mixture was filtered through a frit to give a light-yellow solution. The crude material was purified by preparative HPLC under acidic or basic condition to give the final product.

General Protocol B. A mixture of carboxylic acid (0.082 mmol), EDC (0.082 mmol), HOBt (0.082 mmol), DMAP (0.082 mmol), and

amine (0.163 mmol) in DMF (1.50 mL) was heated in a microwave at 100 °C for 1.5 h. The crude material was purified by preparative HPLC to give the final product.

General Protocol C. A solution of 4-(4-bromophenyl)-2-(piperazin-1-yl)thiazole (0.093 mmol) and Et$_3$N (0.139 mmol) in CH$_2$Cl$_2$ (2.00 mL) was treated at 0 °C with carboxylic chloride or sulfonyl chloride (0.111 mmol). The reaction mixture was allowed to warm to room temperature, stirred for 1 h, and concentrated in vacuo. The crude material was purified by preparative HPLC to give the final product.

1-(4-(4-Bromophenyl)thiazol-2-yl)piperidine-4-carboxamide (2). A general protocol for amination: A mixture of 2,4-dibromothiazole (2.06 g, 8.48 mmol), piperidine-4-carboxamide (1.30 g, 10.1 mmol), and Et$_3$N (2.50 mL) in ethanol (5.00 mL) was heated in a microwave at 100 °C for 1 h. The reaction mixture was cooled to room temperature, diluted with water, and extracted with a mixture of MeOH and CH$_2$Cl$_2$. The organic layer was separated, dried with Na$_2$SO$_4$, and concentrated as a light-brown solid. The crude mixture was purified by Biotage with 0−10% of MeOH in CH$_2$Cl$_2$ with 1% Et$_3$N to give 2.08 g (85%) of 1-(4-bromothiazol-2-yl)piperidine-4-carboxamide as a white solid. ^{1}H NMR (400 MHz, DMSO-d_6) δ ppm 7.31 (br s, 1 H), 6.85 (s, 1 H), 6.82 (br s, 1 H), 3.77−3.90 (m, 2 H), 3.03 (td, J = 12.5, 2.8 Hz, 2 H), 2.29−2.39 (m, 1 H), 1.78 (dd, J = 13.5, 3.1 Hz, 2 H), 1.50−1.63 (m, 2 H). LCMS RT = 4.13 min, m/z 289.9 [M + H$^+$]. The title compound was prepared according to the general protocol A: ^{1}H NMR (400 MHz, DMSO-d_6) δ 7.83−7.79 (m, 2 H), 7.59−7.55 (m, 2 H), 7.33 (s, 1 H), 7.32 (br s, 1 H), 6.82 (br s, 1 H), 3.96 (br. d., J = 12.8 Hz, 2 H), 3.06 (td, J = 12.6, 2.9 Hz, 2 H), 2.36 (tt, J = 11.6, 3.8 Hz, 1 H), 1.82 (dd, J = 13.0, 2.6 Hz, 2 H), 1.61 (qd, J = 12.4, 4.0 Hz, 2 H); LCMS RT = 5.16 min, m/z 366.0 [M + H$^+$]; HRMS (ESI) m/z calcd for C$_{15}$H$_{17}$^{79}BrN$_3$OS [M + H$^+$] 366.0276, found 366.0272.

1-(4-(4-Bromophenyl)thiazol-2-yl)-N-methylpiperidine-4-carboxamide (6a). The compound was prepared according to the general protocol B as a TFA salt. ^{1}H NMR (400 MHz, CDCl$_3$) δ ppm 7.60−7.71 (m, 2 H), 7.47−7.57 (m, 2 H), 6.72 (s, 1 H), 5.78 (br s, 1 H), 4.15 (dt, J = 13.3, 3.5 Hz, 2 H), 3.10−3.30 (m, 2 H), 2.84 (d, J = 5.1 Hz, 3 H), 2.41 (tt, J = 11.1, 3.8 Hz, 1 H), 1.95−2.05 (m, 2 H), 1.81−1.95 (m, 2 H). ^{19}F NMR (376 MHz, CDCl$_3$) δ ppm −75.97 (s). LCMS RT = 5.34 min, m/z 380.0 [M + H$^+$]. HRMS (ESI) m/z calcd for C$_{16}$H$_{19}$^{79}BrN$_3$OS [M + H$^+$] 380.0432, found 380.0425.

1-(4-(4-Bromophenyl)thiazol-2-yl)piperidine-4-carboxylic acid (6k). A solution of ethyl 1-(4-(4-bromophenyl)thiazol-2-yl)-piperidine-4-carboxylate (3.34 g, 8.45 mmol) in THF (24.0 mL) and H$_2$O (8.00 mL) was treated at room temperature with LiOH (1.01 g, 42.2 mmol). The reaction mixture was stirred at room temperature for 24 h, diluted with 100 mL of CH$_2$Cl$_2$, and washed with 2.0 N HCl (25.0 mL). The organic layer was separated, dried with Na$_2$SO$_4$, and concentrated to give a yellow oil. The crude product was purified by Biotage with 0−15% of MeOH in CH$_2$Cl$_2$ to give 2.79 g (90%) of product as a white solid. A small amount of sample was repurified by preparative HPLC under acidic condition to give the product as a TFA salt. ^{1}H NMR (400 MHz, DMSO-d_6) δ ppm 7.74−7.88 (m, 2 H), 7.50−7.64 (m, 2 H), 7.33 (s, 1 H), 3.90 (dt, J = 12.7, 3.5 Hz, 2 H), 3.04−3.23 (m, 2 H), 2.51−2.59 (m, 1 H), 1.94 (dd, J = 13.1, 3.7 Hz, 2 H), 1.51−1.75 (m, 2 H). ^{19}F NMR (376 MHz, DMSO-d_6) δ ppm −74.87 (s). LCMS RT = 5.84 min, m/z 367.0 [M + H$^+$]. HRMS (ESI) m/z calcd for C$_{15}$H$_{16}$^{79}BrN$_2$O$_2$S [M + H$^+$] 367.0116, found 367.0103.

2-(4-(1H-Tetrazol-5-yl)piperidin-1-yl)-4-(4-bromophenyl)-thiazole (6m). A solution of 1-(4-(4-bromophenyl)thiazol-2-yl)-piperidine-4-carbonitrile (59.5 mg, 0.171 mmol) in water (1.00 mL) and 1,4-dioxane (0.58 mL) was treated at room temperature with sodium azide (33.3 mg, 0.513 mmol) and zinc bromide (57.7 mg, 0.256 mmol). The pH value of the solution was adjusted to about 7 with 1 N NaOH (∼6 drops). The reaction mixture was heated in oil bath at 120 °C for

60 h. Another aliquot of reagents was added to the reaction solution, and the mixture was reheated at 120 °C for additional 60 h. The reaction mixture was cooled to room temperature, diluted with EtOAc, and washed with H$_2$O. The organic layer was separated, dried with Na$_2$SO$_4$, and concentrated in vacuo. The crude product was purified by preparative HPLC under basic condition to give 15.0 mg (22%) of product. ^{1}H NMR (400 MHz, DMSO-d_6) δ ppm 7.76−7.87 (m, 2 H), 7.53−7.62 (m, 2 H), 7.33 (s, 1 H), 3.97 (dt, J = 13.2, 3.7 Hz, 2 H), 3.20−3.30 (m, 2 H), 3.14 (tt, J = 11.1, 3.6 Hz, 1 H), 2.04 (dd, J = 13.3, 3.1 Hz, 2 H), 1.71−1.87 (m, 2 H). LCMS RT = 5.62 min, m/z 391.0 [M + H$^+$]. HRMS (ESI) m/z calcd for C$_{15}$H$_{16}$^{79}BrN$_6$S [M + H$^+$] 391.0341, found 391.0338.

1-(4-(4-Bromophenyl)thiazol-2-yl)piperidin-4-amine (6n). A solution of tert-butyl 1-(4-(4-bromophenyl)thiazol-2-yl)piperidin-4-ylcarbamate (78.7 mg, 0.180 mmol) in CH$_2$Cl$_2$ (2.00 mL) was treated at 0 °C with TFA (1.00 mL). The reaction mixture was stirred at 0 °C for 30 min and at room temperature for additional 10 min. The solvents were removed in vacuo. The crude product was filtered through a short cartridge column to remove TFA to give 43.4 mg (72%) of product as a white solid. A small portion of sample was repurified by preparative HPLC under acidic condition to give the final product as a TFA salt. ^{1}H NMR (400 MHz, DMSO-d_6) δ ppm 7.93 (br s, 2 H), 7.72−7.85 (m, 2 H), 7.50−7.65 (m, 2 H), 7.37 (s, 1 H), 4.00 (d, 2 H), 3.25−3.35 (m, 1 H), 3.14 (td, J = 12.8, 2.6 Hz, 2 H), 1.99 (dd, J = 12.6, 3.0 Hz, 2 H), 1.57 (qd, J = 12.4, 4.4 Hz, 2 H). ^{19}F NMR (376 MHz, DMSO-d_6) δ ppm −73.54 (s). LCMS RT = 4.66 min, m/z 338.0 [M + H$^+$]. HRMS (ESI) m/z calcd for C$_{14}$H$_{17}$^{79}BrN$_3$S [M + H$^+$] 338.0327, found 338.0323.

1-(4-(4-(4-Bromophenyl)thiazol-2-yl)piperazin-1-yl)ethanone (6t). The compound was prepared according to the general protocol C as a TFA salt. ^{1}H NMR (400 MHz, CDCl$_3$) δ ppm 7.64−7.74 (m, 2 H), 7.47−7.55 (m, 2 H), 6.82 (s, 1 H), 3.77−3.92 (m, 2 H), 3.66 (br s, 4 H), 3.48−3.58 (m, 2 H), 2.20 (s, 3 H). ^{19}F NMR (376 MHz, DMSO-d_6) δ ppm −76.04 (s). LCMS RT = 5.89 min, m/z 366.0 [M + H$^+$]. HRMS (ESI) m/z calcd for C$_{15}$H$_{17}$^{79}BrN$_3$OS [M + H$^+$] 366.0276, found 366.0274.

4-(4-(4-Bromophenyl)thiazol-2-yl)piperazine-1-carboxamide (6u). A solution of 4-(4-bromophenyl)-2-(piperazin-1-yl)thiazole (40.0 mg, 0.123 mmol) in H$_2$O (2.00 mL) was treated at room temperature with KOCN (20.0 mg, 0.247 mmol). The reaction mixture was stirred at room temperature overnight and extracted with EtOAc. The organic layer was separated, dried with Na$_2$SO$_4$, and concentrated in vacuo. The crude mixture was purified by preparative HPLC under basic condition to give 14.2 mg (31%) of product. ^{1}H NMR (400 MHz, DMSO-d_6) δ ppm 7.82 (d, J = 8.4 Hz, 2 H), 7.57 (d, J = 8.4 Hz, 2 H), 7.37 (s, 1 H), 6.11 (br s, 2 H), 3.37−3.57 (m, 8 H). LCMS RT = 5.33 min, m/z 367.0 [M + H$^+$]. HRMS (ESI) m/z calcd for C$_{14}$H$_{16}$^{79}BrN$_4$OS [M + H$^+$] 367.0228, found 367.0215.

1-(4-(3-Isopropoxyphenyl)pyrimidin-2-yl)piperidine-4-carboxamide (7g). The compound was prepared according to the general protocol A as a TFA salt. ^{1}H NMR (400 MHz, DMSO-d_6) δ ppm 8.41 (d, J = 5.1 Hz, 1 H), 7.66 (ddd, J = 8.1, 1.3, 1.0 Hz, 1 H), 7.57−7.63 (m, 1 H), 7.41 (t, J = 7.9 Hz, 1 H), 7.29 (br s, 1 H), 7.19 (d, J = 5.3 Hz, 1 H), 7.03−7.13 (m, 1 H), 6.78 (br s, 1 H), 4.55−4.84 (m, 3 H), 2.88−3.10 (m, 2 H), 2.41 (tt, J = 11.5, 3.8 Hz, 1 H), 1.80 (dd, J = 12.7, 2.9 Hz, 2 H), 1.50 (qd, J = 12.4, 3.9 Hz, 2 H), 1.30 (d, J = 6.1 Hz, 6 H). ^{19}F NMR (376 MHz, DMSO-d_6) δ ppm −74.96 (s). LCMS RT = 4.45 min, m/z 341.2 [M + H$^+$]. HRMS (ESI) m/z calcd for C$_{19}$H$_{25}$N$_4$O$_2$ [M + H$^+$] 341.1978, found 341.1983.

1-(4-(3,4-Dihydro-2H-benzo[b][1,4]dioxepin-7-yl)pyrimidin-2-yl)piperidine-4-carboxamide (7h). The compound was prepared according to the general protocol A. ^{1}H NMR (400 MHz, DMSO-d_6) δ ppm 8.36 (d, J = 5.1 Hz, 1 H), 7.62−7.80 (m, 2 H), 7.29 (br s, 1 H), 7.01−7.14 (m, 2 H), 6.78 (br s, 1 H), 4.63−4.84 (m, 2 H), 4.10−4.26 (m, 4 H), 2.93 (td, J = 12.7, 2.5 Hz, 2 H), 2.40 (tt, J = 11.5, 3.7 Hz, 1 H), 2.14

(quin, J = 5.6 Hz, 2 H), 1.79 (dd, J = 12.9, 2.7 Hz, 2 H), 1.49 (qd, J = 12.4, 4.3 Hz, 2 H). LCMS RT = 3.84 min, m/z 355.2 [M + H$^+$]. HRMS (ESI) m/z calcd for C$_{19}$H$_{23}$N$_4$O$_3$ [M + H$^+$] 355.1770, found 355.1770.

1-(5-(3,4-Dihydro-2H-benzo[b][1,4]dioxepin-7-yl)thiazol-2-yl)piperidine-4-carboxamide (8a). The compound was prepared according to the general protocol A. ^{1}H NMR (400 MHz, DMSO-d_6) δ ppm 7.47 (s, 1 H), 7.31 (br s, 1 H), 7.07 (d, J = 2.3 Hz, 1 H), 6.97–7.04 (m, 1 H), 6.89–6.96 (m, 1 H), 6.82 (br s, 1 H), 4.12 (dt, J = 9.3, 5.5 Hz, 4 H), 3.89 (dt, J = 12.8, 3.3 Hz, 2 H), 3.04 (td, J = 12.5, 2.9 Hz, 2 H), 2.36 (tt, J = 11.5, 3.7 Hz, 1 H), 2.02–2.15 (m, 2 H), 1.79 (dd, J = 13.2, 2.8 Hz, 2 H), 1.50–1.68 (m, 2 H). LCMS RT = 3.74 min, m/z 360.1 [M + H$^+$]. HRMS (ESI) m/z calcd for C$_{18}$H$_{22}$N$_3$O$_3$S [M + H$^+$] 360.1382, found 360.1379.

1-(5-(3,4-Dihydro-2H-benzo[b][1,4]dioxepin-7-yl)-1,3,4-thiadiazol-2-yl)piperidine-4-carboxamide (8b). The compound was prepared according to the general protocol A as a TFA salt. ^{1}H NMR (400 MHz, DMSO-d_6) δ ppm 7.23–7.52 (m, 3 H), 6.95–7.11 (m, 1 H), 6.84 (br s, 1 H), 4.19 (t, J = 5.6 Hz, 4 H), 3.88 (dt, J = 12.8, 3.5 Hz, 2 H), 3.19 (td, J = 12.4, 2.9 Hz, 2 H), 2.35 (tt, J = 11.4, 4.0 Hz, 1 H), 2.14 (dt, J = 11.2, 5.6 Hz, 2 H), 1.82 (dd, J = 13.5, 2.9 Hz, 2 H), 1.65 (qd, J = 12.4, 3.9 Hz, 2 H). ^{19}F NMR (376 MHz, DMSO-d_6) δ ppm −74.79 (s). LCMS RT = 4.21 min, m/z 361.1 [M + H$^+$]. HRMS (ESI) m/z calcd for C$_{17}$H$_{21}$N$_4$O$_3$S [M + H$^+$] 361.1334, found 361.1332.

1-(5-p-Tolylthiazol-2-yl)piperidine-4-carboxamide (8c). The compound was prepared according to the general protocol A as a TFA salt. ^{1}H NMR (400 MHz, DMSO-d_6) δ ppm 7.58 (s, 1 H), 7.34–7.45 (m, 2 H), 7.32 (br s, 1 H), 7.18 (d, J = 8.0 Hz, 2 H), 6.84 (br s, 1 H), 3.91 (dt, J = 12.9, 3.2 Hz, 2 H), 3.12 (td, J = 12.6, 2.8 Hz, 2 H), 2.38 (tt, J = 11.4, 3.8 Hz, 1 H), 2.29 (s, 3 H), 1.82 (dd, J = 13.2, 2.8 Hz, 2 H), 1.48–1.72 (m, 3 H). ^{19}F NMR (376 MHz, DMSO-d_6) δ ppm −74.86 (s). LCMS RT = 3.91 min, m/z 302.1 [M + H$^+$]. HRMS (ESI) m/z calcd for C$_{16}$H$_{20}$NOS [M + H$^+$] 302.1327, found 302.1328.

1-(5-(3-Isopropoxyphenyl)thiazol-2-yl)piperidine-4-carboxamide (8l). The compound was prepared according to the general protocol A as a TFA salt. ^{1}H NMR (400 MHz, DMSO-d_6) δ ppm 7.65 (s, 1 H), 7.32 (br s, 1 H), 7.24 (t, J = 8.0 Hz, 1 H), 6.93–7.03 (m, 2 H), 6.83 (br s, 1 H), 6.76–6.81 (m, 1 H), 4.55–4.75 (m, 1 H), 3.91 (dt, J = 12.8, 3.4 Hz, 2 H), 3.11 (td, J = 12.5, 2.9 Hz, 2 H), 2.37 (tt, J = 11.4, 3.7 Hz, 1 H), 1.81 (dd, J = 13.3, 2.9 Hz, 2 H), 1.52–1.68 (m, 2 H), 1.26 (d, J = 6.1 Hz, 6 H). ^{19}F NMR (376 MHz, DMSO-d_6) δ ppm −74.91 (s). LCMS RT = 4.30 min, m/z 346.1 [M + H$^+$]. HRMS (ESI) m/z calcd for C$_{18}$H$_{24}$N$_3$O$_2$S [M + H$^+$] 346.1589, found 346.1593.

1-(5-(4-(Methylthio)phenyl)thiazol-2-yl)piperidine-4-carboxamide (8m). The compound was prepared according to the general protocol A as a TFA salt: ^{1}H NMR (400 MHz, DMSO-d_6) δ ppm 7.58 (s, 1 H), 7.37–7.45 (m, 2 H), 7.32 (br s, 1 H), 7.21–7.29 (m, 2 H), 6.83 (br s, 1 H), 3.91 (dt, J = 12.9, 3.0 Hz, 2 H), 3.09 (td, J = 12.5, 2.8 Hz, 2 H), 2.48 (s, 3 H), 2.37 (tt, J = 11.6, 4.0 Hz, 1 H), 1.81 (dd, J = 13.5, 3.5 Hz, 2 H), 1.54–1.67 (m, 2 H). ^{19}F NMR (376 MHz, DMSO-d_6) δ ppm −74.56 (s); LCMS RT = 4.07 min, m/z 361.1 [M + H$^+$]. HRMS (ESI) m/z calcd for C$_{16}$H$_{20}$N$_3$OS$_2$ [M + H$^+$] 334.1048, found 334.1048.

1-(5-(3,4-Dihydro-2H-benzo[b][1,4]dioxepin-7-yl)thiazol-2-yl)piperidine-4-carboxylic acid (9a). A solution of ethyl 1-(5-(3,4-dihydro-2H-benzo[b][1,4]dioxepin-7-yl)thiazol-2-yl)piperidine-4-carboxylate (284 mg, 0.72 mmol) in THF (6.00 mL) and H$_2$O (2.00 mL) was treated at room temperature with LiOH (86.0 mg, 3.60 mmol). The reaction mixture was stirred at room temperature for 24 h, diluted with 100 mL of CH$_2$Cl$_2$, and washed with 2 N HCl (25.0 mL). The organic layer was separated, dried with Na$_2$SO$_4$, and concentrated as a yellow oil. The crude product was purified by Biotage with 0–15% of MeOH in CH$_2$Cl$_2$ to give 233 mg (90%) of product as a white solid. ^{1}H NMR (400 MHz, DMSO-d_6) δ ppm 12.32 (br s, 1 H), 7.48 (s, 1 H), 7.07 (d, J = 2.2

Hz, 1 H), 6.97–7.03 (m, 1 H), 6.89–6.96 (m, 1 H), 4.12 (dt, J = 9.2, 5.5 Hz, 4 H), 3.83 (ddd, J = 13.2, 3.7, 3.5 Hz, 2 H), 2.98–3.20 (m, 2 H), 2.51–2.57 (m, 1 H), 2.04–2.17 (m, 2 H), 1.87–1.98 (m, 2 H), 1.49–1.69 (m, 2 H). LCMS RT = 4.18 min, m/z 361.1 [M + H$^+$]. HRMS (ESI) m/z calcd for C$_{18}$H$_{21}$N$_2$O$_4$S [M + H$^+$] 361.1222, found 361.1221.

1-(5-(3,4-Dihydro-2H-benzo[b][1,4]dioxepin-7-yl)thiazol-2-yl)-N-phenylpiperidine-4-carboxamide (9c). The compound was prepared according to the general protocol A. ^{1}H NMR (400 MHz, DMSO-d_6) δ ppm 9.95 (s, 1 H), 7.60 (dd, J = 8.7, 1.1 Hz, 2 H), 7.49 (s, 1 H), 7.24–7.33 (m, 2 H), 6.97–7.11 (m, 3 H), 6.92–6.97 (m, 1 H), 4.13 (dt, J = 9.4, 5.5 Hz, 4 H), 3.90–4.03 (m, 2 H), 3.10 (td, J = 12.6, 2.7 Hz, 2 H), 2.62 (tt, J = 11.5, 3.7 Hz, 1 H), 2.10 (quin, J = 5.4 Hz, 2 H), 1.90 (dd, J = 13.0, 2.8 Hz, 2 H), 1.71 (qd, J = 12.4, 4.3 Hz, 2 H). LCMS RT = 4.94 min, m/z 436.2 [M + H$^+$]. HRMS (ESI) m/z calcd for C$_{24}$H$_{26}$N$_3$O$_3$S [M + H$^+$] 436.1695, found 436.1699.

■ ASSOCIATED CONTENT

Ⓢ Supporting Information. Assay protocols, experimental procedures, and spectroscopic data (^{1}H NMR, LCMS, and HRMS) are listed for all compounds. This material is available free of charge via the Internet at http://pubs.acs.org.

■ AUTHOR INFORMATION

Corresponding Author
*For J.J.M.: phone, 301-217-9198; fax, 301-217-5736; E-mail, maruganj@mail.nih.gov. For J.X.: E-mail, xiaoj@mail.nih.gov.

Present Addresses
§Department of Dermatology, Indiana University School of Medicine, 980 West Walnut Street, Indianapolis, Indiana 46202.

■ ABBREVIATIONS USED

SMA, spinal muscular atrophy; SMN, survival motor neuron; *SMN1*, survival motor neuron gene 1; *SMN2*, survival motor neuron gene 2; qHTS, quantitative high-throughput screen; ROI, rate of induction; NIH, National Institutes of Health; RNA, ribonucleic acid; snRNP, small nuclear ribonucleoproteins; mRNA, messenger RNA; SAR, structure—activity relationships; SPR, structure—property relationships; PK, pharmacokinetics; PBA, sodium 4-phenylbutyrate; FDA, U.S. Food and Drug Administration; cDNA, complementary DNA; DMSO, dimethyl sulfoxide; MLSMR, Molecular Libraries-Small Molecule Repository; GFP, green fluorescent protein; P-gp, P-glycoprotein; MCPBA, *meta*-chloroperoxybenzoic acid; HPLC, high-performance liquid chromatography; RT-PCR, real-time polymerase chain reaction; HDAC, histone deacetylases; DcpS, decapping enzyme scavenger; SMNΔ7, delete exon 7 SMN protein; ADME, absorption, distribution, metabolism, and excretion; CNS, central nervous system;

HRP, horseradish peroxidase; HEK-293, human embryonic kidney 293; DMEM, Dulbecco's Modified Eagle Medium; FCS, fetal calf serum; CCD, charge-coupled device; TLC, thin layer chromatography; DMF, dimethylformamide; EDC, 1-ethyl-3-(3-dimethylaminopropyl)carbodiimide; HOBt, hydroxybenzotriazole; DMAP, 4-dimethylaminopyridine; TEA, triethylamine; TFA, trifluoroacetic acid.

■ REFERENCES

(1) (a) Roberts, D. F.; Chavez, J.; Court, S. D. The genetic component in child mortality. *Arch. Dis. Child.* **1970**, *45*, 33–38. (b) Crawford, T. O.; Pardo, C. A. The neurobiology of childhood spinal muscular atrophy. *Neurobiol. Dis.* **1996**, *3*, 97–110.

(2) Pearn, J. Incidence, prevalence, and gene frequency studies of chronic childhood spinal muscular atrophy. *J. Med. Genet.* **1978**, *15*, 409–413.

(3) (a) www.fsma.org. (b) Pearn, J. Classification of spinal muscular atrophies. *Lancet* **1980**, *1*, 919–922.

(4) Lefebvre, S.; Burglen, L.; Reboullet, S.; Clermont, O.; Burlet, P.; Viollet, L.; Benichou, B.; Cruaud, C.; Millasseau, P.; Zeviani, M.; Le Paslier, D.; Frezal, J.; Cohen, D.; Weissenbach, J.; Munnich, A.; Melki, J. Identification and characterization of a spinal muscular atrophy-determining gene. *Cell* **1995**, *80*, 155–165.

(5) Lefebvre, S.; Burlet, P.; Liu, Q.; Bertrandy, S.; Clermont, O.; Munnich, A.; Dreyfuss, G.; Melki, J. Correlation between severity and SMN protein level in spinal muscular atrophy. *Nature Genet.* **1997**, *16*, 265–269.

(6) (a) Lorson, C. L.; Hahnen, E.; Androphy, E. J.; Wirth, B. A single nucleotide in the SMN gene regulates splicing and is responsible for spinal muscular atrophy. *Proc. Natl. Acad. Sci. U.S.A.* **1999**, *96*, 6307–6311. (b) Monani, U. R.; Lorson, C. L.; Parsons, D. W.; Prior, T. W.; Androphy, E. J.; Burghes, A. H. M.; McPherson, J. D. A single nucleotide difference that alters splicing patterns distinguishes the SMA gene SMN1 from the copy gene SMN2. *Hum. Mol. Genet.* **1999**, *8*, 1177–1183.

(7) Lorson, C. L.; Strasswimmer, J.; Yao, J. M.; Baleja, J. D.; Hahnen, E.; Wirth, B.; Le, T. T.; Burghes, A. H. M.; Androphy, E. J. SMN oligomerization defect correlates with spinal muscular atrophy severity. *Nature Genet.* **1998**, *19*, 63–66.

(8) (a) Feldkotter, M.; Schwarzer, V.; Wirth, R.; Wienker, T. F.; Wirth, B. Quantitative analyses of SMN1 and SMN2 based on real-time light Cycler PCR: fast and highly reliable carrier testing and prediction of severity of spinal muscular atrophy. *Am. J. Hum. Genet.* **2002**, *70*, 358–368. (b) McAndrew, P. E.; Parsons, D. W.; Simard, L. R.; Rochette, C.; Ray, P. N.; Mendell, J. R.; Prior, T. W.; Burghes, A. H. M. Identification of proximal spinal muscular atrophy carriers and patients by analysis of SMNT and SMNC gene copy number. *Am. J. Hum. Genet.* **1997**, *60*, 1411–1422.

(9) Pellizzoni, L.; Baccon, J.; Charroux, B.; Dreyfuss, G. The survival of motor neurons (SMN) protein interacts with the snoRNP proteins fibrillarin and GAR1. *Curr. Biol.* **2001**, *11*, 1079–1088.

(10) Foust, K. D.; Wang, X.; McGovern, V. L.; Braun, L.; Bevan, A. K.; Haidet, A. M.; Le, T. T.; Morales, P. R.; Rich, M. M.; Burghes, A. H. M.; Kaspar, B. K. Rescue of the spinal muscular atrophy phenotype in a mouse model by early postnatal delivery of SMN. *Nature Biotechnol.* **2010**, *28*, 271–274.

(11) (a) Hua, Y.; Sahashi, K.; Hung, G.; Rigo, F.; Passini, M. A.; Bennett, C. F.; Krainer, A. R. Antisense correction of SMN2 splicing in the CNS rescues necrosis in a type III SMA mouse model. *Genes Dev.* **2010**, *24*, 1634–1644. (b) Aartsma-Rus, A.; van Ommen, G.-J. B. Progress in therapeutic antisense applications for neuromuscular disorders. *Eur. J. Hum. Genet.* **2010**, *18*, 146–153.

(12) Deshpande, D. M.; Kim, Y. S.; Martinez, T.; Carmen, J.; Dike, S.; Shats, I.; Rubin, L. L.; Drummond, J.; Krishnan, C.; Hoke, A.; Maragakis, N.; Shefner, J.; Rothstein, J. D.; Kerr, D. A. Recovery from paralysis in adult rats using embryonic stem cells. *Ann. Neurol.* **2006**, *60*, 32–44.

(13) Lunn, M. R.; Stockwell, B. R. Chemical genetics and orphan genetic diseases. *Chem. Biol.* **2005**, *12*, 1063–1073.

(14) Chang, J.-G.; Hsieh-Li, H.-M.; Jong, Y.-J.; Wang, N. M.; Tsai, C.-H.; Li, H. Treatment of spinal muscular atrophy by sodium butyrate. *Proc. Natl. Acad. Sci. U.S.A.* **2001**, *98*, 9808–9813.

(15) Andreassi, C.; Angelozzi, C.; Tiziano, F. D.; Vitali, T.; Vincenzi, E. D.; Boninsegna, A.; Villanova, M.; Bertini, E.; Pini, A.; Neri, G.; Brahe, C. Phenylbutyrate increases SMN expression in vitro: relevance for treatment of spinal muscular atrophy. *Eur. J. Hum. Genet.* **2004**, *12*, 59–65.

(16) Grzeschik, S. M.; Ganta, M.; Prior, T. W.; Heavlin, W. D.; Wang, C. H. Hydroxyurea enhances SMN2 gene expression in spinal muscular atrophy cells. *Ann. Neurol.* **2005**, *58*, 194–202.

(17) Wirth, B.; Riessland, M.; Hahnen, E. Drug discovery for spinal muscular atrophy. *Expert Opin. Drug Discovery* **2007**, *2*, 437–451.

(18) (a) Brichta, L.; Hofmann, Y.; Hahnen, E.; Siebzehnrubl, F. A.; Raschke, H.; Blumcke, I.; Eyupoglu, I. Y.; Wirth, B. Valproic acid increases the SMN2 protein level: a well-known drug as a potential therapy for spinal muscular atrophy. *Hum. Mol. Genet.* **2003**, *12*, 2481–2489. (b) Sumner, C. J.; Huynh, T. N.; Markowitz, J. A.; Perhac, J. S.; Hill, B.; Coovert, D. D.; Schussler, K.; Chen, X.; Jarecki, J.; Burghes, A. H. M.; Taylor, J. P.; Fischbeck, K. H. Valproic acid increases SMN levels in spinal muscular atrophy patient cells. *Ann. Neurol.* **2003**, *54*, 647–654.

(19) Andreassi, C.; Jarecki, J.; Zhou, J.; Coovert, D. D.; Monani, U. R.; Chen, X.; Whitney, M.; Pollok, B.; Zhang, M.; Androphy, E. J.; Burghes, A. H. M. Aclarubicin treatment restores SMN levels to cells derived from type I spinal muscular atrophy patients. *Hum. Mol. Genet.* **2001**, *10*, 2841–2849.

(20) Wolstencroft, E. C.; Mattis, V.; Bajer, A. A.; Young, P. J.; Lorson, C. L. A non-sequence-specific requirement for SMN protein activity: the role of aminoglycosides in inducing elevated SMN protein levels. *Hum. Mol. Genet.* **2005**, *14*, 1199–1210.

(21) Avila, A. M.; Burnett, B. G.; Taye, A. A.; Gabanella, F.; Knight, M. A.; Hartenstein, P.; Cizman, Z.; Di Prospero, N. A.; Pellizzoni, L.; Fischbeck, K. H.; Sumner, C. J. Trichostatin A increases SMN expression and survival in a mouse model of spinal muscular atrophy. *J. Clin. Invest.* **2007**, *117*, 659–671.

(22) (a) Hahnen, E.; Eyupoglu, I. Y.; Brichta, L.; Haastert, K.; Trankle, C.; Siebzehnrubl, F. A.; Riessland, M.; Holker, I.; Claus, P.; Romstock, J.; Buslei, R.; Wirth, B.; Blumcke, I. In vitro and ex vivo evaluation of second-generation histone deacetylase inhibitors for the treatment of spinal muscular atrophy. *J. Neurochem.* **2006**, *98*, 193–202. (b) Riessland, M.; Ackermann, B.; Forster, A.; Jakubik, M.; Hauke, J.; Garbes, L.; Fritzsche, I.; Mende, Y.; Blumcke, I.; Hahnen, E.; Wirth, B. SAHA ameliorates the SMA phenotype in two mouse models for spinal muscular atrophy. *Hum. Mol. Genet.* **2010**, *19*, 1492–1506.

(23) Yuo, C.-Y.; Lin, H.-H.; Chang, Y.-S.; Yang, W.-K.; Chang, J.-G. 5-(N-Ethyl-N-isopropyl)-amiloride enhances SMN2 exon 7 inclusion and protein expression in spinal muscular atrophy cells. *Ann. Neurol.* **2008**, *63*, 26–34.

(24) Garbes, L.; Riessland, M.; Hölker, I.; Heller, R.; Hauke, J.; Tränkle, C.; Coras, R.; Blümcke, I.; Hahnen, E.; Wirth, B. LBH589 induces up to 10-fold SMN protein levels by several independent mechanisms and is effective even in cells from SMA patients nonresponsive to valproate. *Hum. Mol. Genet.* **2009**, *18*, 3645–3658.

(25) Dayangac-Erden, D.; Bora, G.; Ayhan, P.; Kocaefe, C.; Dalkara, S.; Yelekci, K.; Demir, A. S.; Erdem-Yurter, H. Histone deacetylase inhibition activity and molecular docking of (E)-Resveratrol: its therapeutic potential in spinal muscular atrophy. *Chem. Biol. Drug Des.* **2009**, *73*, 355–364.

(26) Lunn, M. R.; Root, D. E.; Martino, A. M.; Flaherty, S. P.; Kelley, B. P.; Coovert, D. D.; Burghes, A. H. M.; thi Man, N.; Morris, G. E.; Zhou, J.; Androphy, E. J.; Sumner, C. J.; Stockwell, B. R. Indoprofen upregulates the survival motor neuron protein through a cyclooxygenase-independent mechanism. *Chem. Biol.* **2004**, *11*, 1489–1493.

(27) Hastings, M. L.; Berniac, J.; Liu, Y. H.; Abato, P.; Jodelka, F. M.; Barthel, L.; Kumar, S.; Dudley, C.; Nelson, M.; Larson, K.; Edmonds, J.;

Bowser, T.; Draper, M.; Higgins, P.; Krainer, A. R. Tetracyclines that promote *SMN2* exon 7 splicing as therapeutics for spinal muscular atrophy. *Sci. Transl. Med.* **2009**, *1*, 5ra12.

(28) Jarecki, J.; Chen, X.; Bernardino, A.; Coovert, D. D.; Whitney, M.; Burghes, A. H. M.; Stack, J.; Pollok, B. A. Diverse small-molecule modulators of SMN expression found by high-throughput compound screening: early leads towards a therapeutic for spinal muscular atrophy. *Hum. Mol. Genet.* **2005**, *14*, 2003–2018.

(29) (a) Thurmond, J.; Butchbach, M. E.; Palomo, M.; Pease, B.; Rao, M.; Bedell, L.; Keyvan, M.; Pai, G.; Mishra, R.; Haraldsson, M.; Andresson, T; Bragason, G.; Thosteinsdottir, M.; Bjornsson, J. M.; Coovert, D. D.; Burghes, A. H. M.; Gurney, M. E.; Singh, J. Synthesis and biological evaluation of novel 2,4-diaminoquinazoline derivatives as *SMN2* promoter activators for the potential treatment of spinal muscular atrophy. *J. Med. Chem.* **2008**, *51*, 449–469. (b) Singh, J.; Salcius, M.; Liu, S. W.; Staker, B. L.; Mishra, R.; Thurmond, J.; Michaud, G.; Mattoon, D. R.; Printen, J.; Christensen, J.; Bjornsson, J. M.; Pollok, B. A.; Kiledjian, M.; Stewart, L.; Jarecki, J.; Gurney, M. E. DcpS as a therapeutic target for spinal muscular atrophy. *ACS Chem. Biol.* **2008**, *3*, 711–722.

(30) Butchbach, M. E.; Singh, J.; Thornorsteinsdóttir, M.; Saieva, L.; Slominski, E.; Thurmond, J.; Andrésson, T.; Zhang, J.; Edwards, J. D.; Simard, L. R.; Pellizzoni, L.; Jarecki, J.; Burghes, A. H. M.; Gurney, M. E. Effects of 2,4-diaminoquinazoline derivatives on SMN expression and phenotype in a mouse model for spinal muscular atrophy. *Hum. Mol. Genet.* **2009**, *19*, 454–467.

(31) Borman, S. Rare and neglected diseases. *Chem. Eng. News* **2010**, *88*, 36–38.

(32) It is interesting to find that both D156844 and another analogue **5g** in ref 29a were not active in our current in-house *SMN2*-luciferase reporter assay.

(33) Zhang, M. L.; Lorson, C. L.; Androphy, E. J.; Zhou, J. An in vivo reporter system for measuring increased inclusion of exon 7 in *SMN2* mRNA: potential therapy of SMA. *Gene Ther.* **2001**, *8*, 1532–1538.

(34) Inglese, J.; Auld, D. S.; Jadhav, A.; Johnson, R. L.; Simeonov, A.; Yasgar, A.; Zheng, W.; Austin, C. P. Quantitative high-throughput screening: A titration-based approach that efficiently identifies biological activities in large chemical libraries. *Proc. Natl. Acad. Sci. U.S.A.* **2006**, *103*, 11473–11478.

(35) Austin, C. P.; Brady, L. S.; Insel, T. R.; Collins, F. S. NIH molecular libraries initiative. *Science* **2004**, *306*, 1138–1139.

(36) All the activities of these compounds in other assays are publicly available in the PubChem (http://pubchem.ncbi.nlm.nih.gov/).

(37) (a) Auld, D. S.; Zhang, Y. Q.; Southall, N. T.; Rai, G.; Landsman, M.; Maclure, J.; Langevin, D.; Thomas, C. J.; Austin, C. P.; Inglese, J. A basis for reduced chemical library inhibition of firefly luciferase obtained from directed evolution. *J. Med. Chem.* **2009**, *52*, 1450–1458. (b) Auld, D. S.; Thorne, N.; Nguyen, D.-T.; Inglese, J. A specific mechanism for nonspecific activation in reporter-gene assays. *ACS Chem. Biol.* **2008**, *3*, 463–470. (c) Auld, D. S.; Thorne, N.; Maguire, W. F.; Inglese, J. Mechanism of PTC124 activity in cell-based luciferase assays of nonsense codon suppression. *Proc. Natl. Acad. Sci. U.S.A.* **2009**, *106*, 3585–3590.

(38) Xia, M.; Huang, R.; Guo, V.; Southall, N.; Cho, M.-H.; Inglese, J.; Austin, C. P.; Nirenberg, M. Identification of compounds that potentiate CREB signaling as possible enhancers of long-term memory. *Proc. Natl. Acad. Sci. U.S.A.* **2009**, *106*, 2412–2417.

(39) All the results for this screening are publicly available in the PubChem (AID no. 488832). Compound **1** was named as **ML104** and compound **8m** was named as **ML200** in the PubChem.

(40) van Breemen, R. B.; Li, Y. Caco-2 cell permeability assays to measure drug absorption. *Expert Opin. Drug Metab. Toxicol.* **2005**, *1*, 175–185.

(41) Aller, S. G.; Yu, J.; Ward, A.; Weng, Y.; Chittaboina, S.; Zhuo, R.; Harrell, P. M.; Trinh, Y. T.; Zhang, Q.; Urbatsch, I. L.; Chang, G. Structure of P-glycoprotein reveals a molecular basis for poly-specific drug binding. *Science* **2009**, *323*, 1718–1722.

(42) Nicolaou, K. C.; He, Y.; Roschangar, F.; King, N. P.; Vourloumis, D.; Li, T. Total synthesis of epothilone E & analogs with modified side chains through the Stille coupling reaction. *Angew. Chem., Int. Ed. Engl.* **1998**, *37*, 84–87.

(43) Miyaura, N.; Suzuki, A. Palladium-catalyzed cross-coupling reactions of organoboron compounds. *Chem. Rev.* **1995**, *95*, 2457–2483.

(44) Jolidon, S.; Narquizian, R.; Norcross, R. D.; Pinard, E. [4-(Heteroaryl)piperazin-1-yl]-(2,5-substituted-phenyl)methanone derivatives as glycine transporter 1 (glyt-1) inhibitors for the treatment of neurological and neuropsychiatric disorders. PCT Patent Application WO2006/72436 A1, 2006.

(45) Palani, A.; Berlin, M. Y.; Aslanian, R. G.; Vaccaro, H. M.; Chan, T.-Y.; Xiao, D.; Degrado, S.; Rao, A. U.; Chen, X.; Lee, Y. J.; Sofolarides, M. J.; Shao, N.; Huang, Y. R.; Liu, Z.; Wang, L. Y.; Pu, H. Pyrrolidine, piperidine and piperazine derivatives and methods of use thereof. PCT Patent Application WO2010/45303 A2, 2010.

(46) Plant, A.; Seitz, T.; Jansen, J. R.; Erdelen, C.; Turberg, A.; Hansen, O. Delta 1-pyrrolines used as pesticides.U.S. Patent Application US2004/82586 A1, 2004.

(47) Sekiguchi, Y.; Kanuma, K.; Omodera, K.; Tran, T.-A.; Semple, G.; Kramer, B. A. Pyrimidine derivatives and methods of treatment related to the use thereof. PCT Patent Application WO/2005/095357, 2005.

(48) Westhuyzen, C. W.; van der; Rousseau, A. L.; Parkinson, C. J. Effect of substituent structure on pyrimidine electrophilic substitution. *Tetrahedron* **2007**, *63*, 5394–5405.

(49) Devasagayaraj, A.; Jin, H.; Liu, Q.; Marinelli, B.; Samala, L.; Shi, Z.-C.; Tunoori, A.; Wang, Y.; Wu, W.; Zhang, C.; Zhang, H. Multicyclic amino acid derivatives and methods of their use. U.S. Patent Application US2007/191370 A1, 2007.

(50) Coovert, D. D.; Le, T. T.; McAndrew, P. E.; Strasswimmer, J.; Crawford, T. O.; Mendell, J. R.; Coulson, S. E.; Androphy, E. J.; Prior, T. W.; Burghes, A. H. M. The survival motor neuron protein in spinal muscular atrophy. *Hum. Mol. Genet.* **1997**, *6*, 1205–1214.